Cold Regions Science and Engineering

Part III, Section A3a

EXPLOSIONS AND SNOW

JUNE 1965

U.S. ARMY MATERIEL COMMAND
COLD REGIONS RESEARCH & ENGINEERING LABORATORY
HANOVER, NEW HAMPSHIRE

DA Project 1V02500A130

Cold Regions Science and Engineering
Part III, Section A3a

EXPLOSIONS AND SNOW

by

Malcolm Mellor

JUNE 1965

U.S. ARMY MATERIEL COMMAND
COLD REGIONS RESEARCH & ENGINEERING LABORATORY
HANOVER, NEW HAMPSHIRE

DA Project 1V02500A130

PREFACE

This monograph summarizes available information on the response of snow to explosions and on the modification of blast effects by snow. The author is grateful to Dr. Andrew Assur, Scientific Advisor, USA CRREL, for a detailed review and helpful discussions. Review comments by U. S. Army Engineer Waterways Experiment Station (USAEWES) are also gratefully acknowledged.

USA CRREL is an Army Materiel Command laboratory.

DA Project IV025001A130
DASA Subtask 02.0462

Errata — Cold Regions Science and Engineering. Part III, Sect. A3a, Explosions and Snow

p. 14, last paragraph, line 4: for "no. 211 " read "no. 231."

p. 26: The sentence beginning on line 6 of the text should read. "Over the entire pressure range 1.0 to 100 psi an inverse square relationship seems a reasonable approximation· it is a good approximation over a limited range centered on 12 psi "

p. 29, paragraph 5 line 5: for "from" read "than."

CONTENTS

ILLUSTRATIONS

CONTENTS (Cont'd)

TABLES

EDITOR'S FOREWORD

"Cold Regions Science and Engineering" consists of a series of monographs summarizing existing knowledge and providing references for the use of professional engineers responsible for design and construction in Cold Regions, defined as those areas of the earth where frost is an essential consideration in engineering.

Sections of the work are being published as they become ready, not necessarily in numerical order, but fitting into this plan:

I. Environment
   - A. General
     1. Geology and physiography
     2. Perennially frozen ground (permafrost)
     3. Climatology
   - B. Regional
     1. The Antarctic ice sheet
     2. The Greenland ice sheet

II. Physical Science
   - A. Geophysics
     1. Heat exchange at the earth's surface
     2. Exploratory geophysics
   - B. The physics and mechanics of snow as a material
   - C. The physics and mechanics of ice
     1. Snow and ice on the earth's surface
     2. Ice as a material
   - D. The physics and mechanics of frozen ground

III. Engineering
   - A. Snow engineering
     1. Engineering properties
     2. Construction
     3. Technology
     4. Oversnow transport
   - B. Ice engineering
   - C. Frozen ground engineering
   - D. General

IV. Miscellaneous

F. J. SANGER

LIST OF SYMBOLS

c_o - Speed of sound in undisturbed air

d - Distance from a source

p - Overpressure. The transient pressure above original ambient pressure during passage of a shock. (Subscript m denotes maximum value, i.e. peak overpressure)

q - Dynamic pressure, or wind pressure. (Subscript m denotes peak value)

r - Radius from a source

t - Time

t_+ - Duration of positive overpressure phase following passage of a shock

u - Particle velocity of air or snow set in motion by an explosion

v - Velocity of an elastic wave

A - Wave amplitude

E - Young's modulus

H - Crater depth

R - Crater radius

V - Crater volume

The following subscripts are used to denote dimensions to different crater limits:

a apparent crater limit
c complete rupture limit
e extreme rupture limit

The additional subscript m denotes a maximum value

I - Impulse ($\int p\,dt$, $\int q\,dt$)

P - Ambient pressure prior to an explosive disturbance

T - Absolute temperature

U - Shock velocity

W - Charge weight, or charge yield

α - Attenuation constant

γ - Snow density

λ - Scaled distance ($lb/ft^{\frac{1}{3}}$)

ν - Poisson's ratio

ρ - Air density

Δ - Depth ratio (dimensionless)

Δ_* - Critical depth (ft)

EXPLOSIONS AND SNOW

by

Malcolm Mellor

The effects of explosions on snow, and conversely the effects of snow on explosions, are matters of some interest. Explosive charges are fired in snow for a variety of technical purposes, and there is always a possibility that explosive weapons might be employed in a snow environment. Although similar in many ways to soils, snow possesses certain properties which are significantly different from those of soils.

Relevant snow properties

Dense, dry snow is a permeable material consisting of an ice matrix with interconnecting air-filled voids. Wet snow is a three-phase material containing ice, water and air. The density of deposited snow ranges from less than 0.2 g/cm^3 up to 0.8 g/cm^3, above which density it becomes impermeable, so that it is regarded as ice rather than snow. The density of firm, dry snow lying near the surface is usually in the range 0.25 to 0.45 g/cm^3. The density of any given layer in a snow deposit increases with time as a result of quasi-viscous creep under body forces. In dense snow, intergranular bonds usually develop, either by melting and refreezing or by dry sintering (age-hardening).

For moderate loads and displacements the ice matrix of snow is viscoelastic; it will sustain elastic vibrations (with viscous damping) and will creep under prolonged loading (the stress/strain-rate relation is non-linear). Under strong triaxial compression snow compacts to high density, while high tensile and shear stresses produce fracture and fragmentation. Intense, high-speed loading, such as is induced by explosions, produces an elastic strain up to some yield point, followed by plastic compression and finally an approach to the incompressible state. It seems certain that the response of snow to explosive loadings will be complicated by pressure transmission in the interstitial air, but the details of this interaction effect are not yet well known.

A snow surface reflects pressure waves from the air, but is virtually unique among inorganic surfaces in that it is significantly different from the ideal rigid reflector commonly assumed in theoretical work.

Snow may be melted or vaporized by thermal energy from an explosion at exposed surfaces, but it seems unlikely that there will be appreciable heat transfer to any great depth, since the periods involved are short. Of the heat transfer processes available, convection may be more significant than radiation or conduction in the solid. Snow is a very efficient reflector for luminous radiation; it also dissipates heat by ablation.

A detailed review of snow properties is given elsewhere[7].

Scaling and normalizing variables

In order to compare the effects of explosions with different energy yields it is convenient to scale linear dimensions, pressures and times according to the yield. It is also useful to be able to relate variables in a general form by curves drawn on dimensionless axes; this is done by normalizing.

The scaling rule, or cube root law.* After an explosion a given pressure occurs at a distance from the source which is proportional to the cube root of the energy yield under suitably similar conditions. Pressure, distance, arrival time, phase duration and impulse can all be scaled according to the cube root law.[2]

The scaling rule can be stated in a general form as

$$\frac{d_2}{d_1} = \frac{t_2}{t_1} = \frac{I_2}{I_1} = \left(\frac{W_2}{W_1}\right)^{\frac{1}{3}} \qquad (1)$$

where d = distance from the center of the explosion (slant range) for a given overpressure

t = arrival time or phase duration at distance d

I = impulse at distance d (impulse is the integral of positive pressure with respect to time during the positive phase)

W = energy yield or equivalent TNT charge weight (1 ton of TNT releases 10^9 calories).

Cube root scaling is not directly applicable for comparing nuclear and "H. E." (high explosive) explosions because of the very different distributions of kinetic and radiant energy; suitable efficiency factors must be employed.

Scaled distance. In comparing linear dimensions for explosions with different yields, scaled (or "reduced") distances are used. Following directly from the scaling rule above, scaled distances (slant range, depth, height, radius) are found by dividing the actual distance by the cube root of the energy yield or charge weight,

$$\text{Scaled distance} = \frac{\text{Actual distance}}{\text{Cube root of yield}} .$$

In the form now used, scaled distances are not dimensionless.† They typically have dimensions $(\text{ft/lb}^{\frac{1}{3}})$ or $(\text{ft/kt}^{\frac{1}{3}})$.**

Normalizing. Variables are normalized in the usual way, dividing the absolute values by some reference value to give a dimensionless number. For example, the time-dependent overpressure at a given point may be divided by the peak overpressure for that point.

The explosion

The sequence of events after detonation of a high explosive charge buried in firm polar snow has been described by Livingston,[6] who marks the following stages:

a. Cavity growth: The gas bubble expands and forms a primary cavity as the surrounding snow is compacted radially. Cavity walls are fractured and an ice skin is formed by fusion. The compacted density of the (unloaded) snow does not exceed 0.6 g/cm^3.††

---

*For an entertaining discussion of scaling, see ref. 5.

†This dimensional difficulty might be overcome by scaling according to "equivalent TNT volume" rather than equivalent TNT weight.

** kt = kiloton

††This is interesting: 0.6 g/cm^3 is about the maximum density which can be achieved by field compaction methods imposing short-duration loadings (see monographs IIIA-1, Properties of snow, and IIIA-2, Construction.

b. Implosion: The primary cavity is said to be disturbed by reversal in the direction of displacement; the ice skin and the compacted snow zone formed during cavity growth are disrupted.

c. Vortex and scouring motions: Implosion is followed by vortex motion within the snow and by a scouring action as the gas bubble emerges from a rising column defined by the vortex.

It is said that during loading of the snow a substantial proportion of the explosive energy is expended in compacting and deforming the material without destroying cohesion, while during unloading much of the energy used to compress intergranular air is recovered and reexpended in fracturing and deforming the material. The failure of the snow is characterized as a "viscous-damping" type of failure. The snow mass is regarded as a cellular dashpot through which displaced air is forced, and it is believed that vibrations are damped by this air motion.

Near the center of the explosion there is a violent disturbance; the snow is vaporized, fused and fragmented. Surrounding this region of total disruption is a zone where the snow is extensively compacted and fractured, but as distance from the explosion increases, permanent deformation of the snow becomes less intense. At a certain radius from the explosion, permanent deformation of the snow ceases to be detectable, and from this radius outwards the snow has responded elastically to the attenuated wave.

In the case of a nuclear explosion the quantity of vapor vented from a subsurface burst in snow or ice might be considerable. Plump[9] points out that in a vented burst where the fireball is wholly contained, about 500 tons of ice would be vaporized by an explosion of 1 kiloton yield, assuming that one-third of the energy goes into heat generation.*

Craters

The crater of an explosion is taken as embracing all of the zone surrounding the explosion in which permanent deformation has occurred. In the sole major study of craters in snow,[6] the following terminology is adopted for describing the principal zones of a crater:

a. The apparent crater, which is immediately visible to the eye.

b. The true crater, or zone of total fragmentation.

c. The complete-rupture zone, which is a zone of fracture and deformation immediately surrounding the true crater.

d. The extreme-rupture zone.† This is a zone containing the most distant snow to be deformed permanently; original bedding is maintained, but minor fracture and displacement have occurred.

Figure 1 shows the limits of these zones diagrammatically.

The above terminology is slightly different from that adopted for description of craters made in soil and rock by nuclear explosions,[2] where the terms "rupture zone" and "plastic zone" are used instead of "complete rupture zone" and "extreme rupture zone" respectively. A crater is often assumed to have a paraboloidal shape, so that the volume is given by $\frac{1}{2}\pi R^2 H$, where R and H are radius and depth of the crater

*Mass of vapor $= \frac{\text{heat energy}}{\text{heat of sublimation}}$. For 1 kt total yield, mass of vapor $= \frac{\frac{1}{3} \times 10^{12}}{670}$ g.

†Livingston's inconsistent term "extreme rupture" has been retained in this review, although it might be better to substitute the words "incomplete rupture."

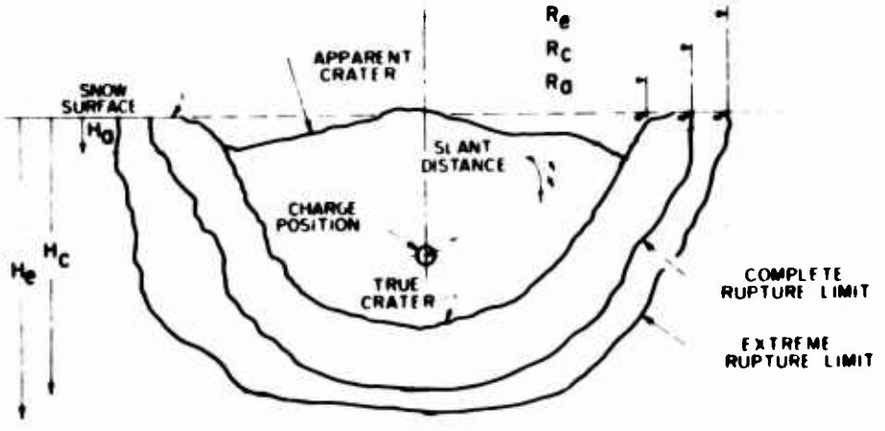

Figure 1. The form of a crater in snow and the terminology used to describe various zones and limits. (After Livingston, ref. 6)

respectively. In snow, however, crater shape may depart considerably from a paraboloid.[6]

For contact nuclear explosions on soil and rock (scaled height or depth of burst not exceeding 5 ft/kt$^{\frac{1}{3}}$), the diameter and depth of the crater are taken as proportional to the cube root of the energy yield of the explosion, while the mass of material ejected is roughly proportional to the yield. The limited high-explosive data for snow were not originally analyzed to give corresponding information; however, the adoption of cube-root scaling implies that the same relation holds, and the present author has related crater dimensions to the cube root of charge yield directly.

For a given charge size, the diameter and depth of the crater increase as the charge depth increases in a limited range, and crater shape varies. Below a certain depth of burial, the snow surface ceases to be displaced by the explosion and all the energy is expended within the snow; such an explosion is known as a camouflet. Figure 2 shows schematically the change of crater size and shape as charge depth is increased.

There is a converse effect for air shots, crater size diminishing as the height of burst increases. It appears that over soil and rock nuclear explosions do not make significant craters if the height of burst exceeds one-tenth of the fireball radius[2]. Over snow, however, it seems probable that craters would be bigger for a given yield and height of burst, since the density of snow is appreciably lower and significant vaporization can occur.

Crater data for snow

The principal source of information on craters in snow is Livingston's report [6] on tests made on the Greenland Ice Cap. The report contains a wealth of data, but further analysis seems desirable. The following statements represent the writer's broad interpretation after limited consideration of the report; some data are necessarily abstracted in the forms used in the original. Limited data for seasonal snow of lower density are given in ref. 1 and 17, and analyzed in ref. 23; Table III summarizes these results.

Charge yield and crater dimensions. It is assumed throughout the Livingston work, as well as in most other cratering studies, that linear dimensions are proportional to the cube root of charge weight. When the actua charge weight is used, as opposed to the TNT equivalent, the coefficient of proportionality varies with the type of explosive. However, effects due to variations in explosive characteristics hardly

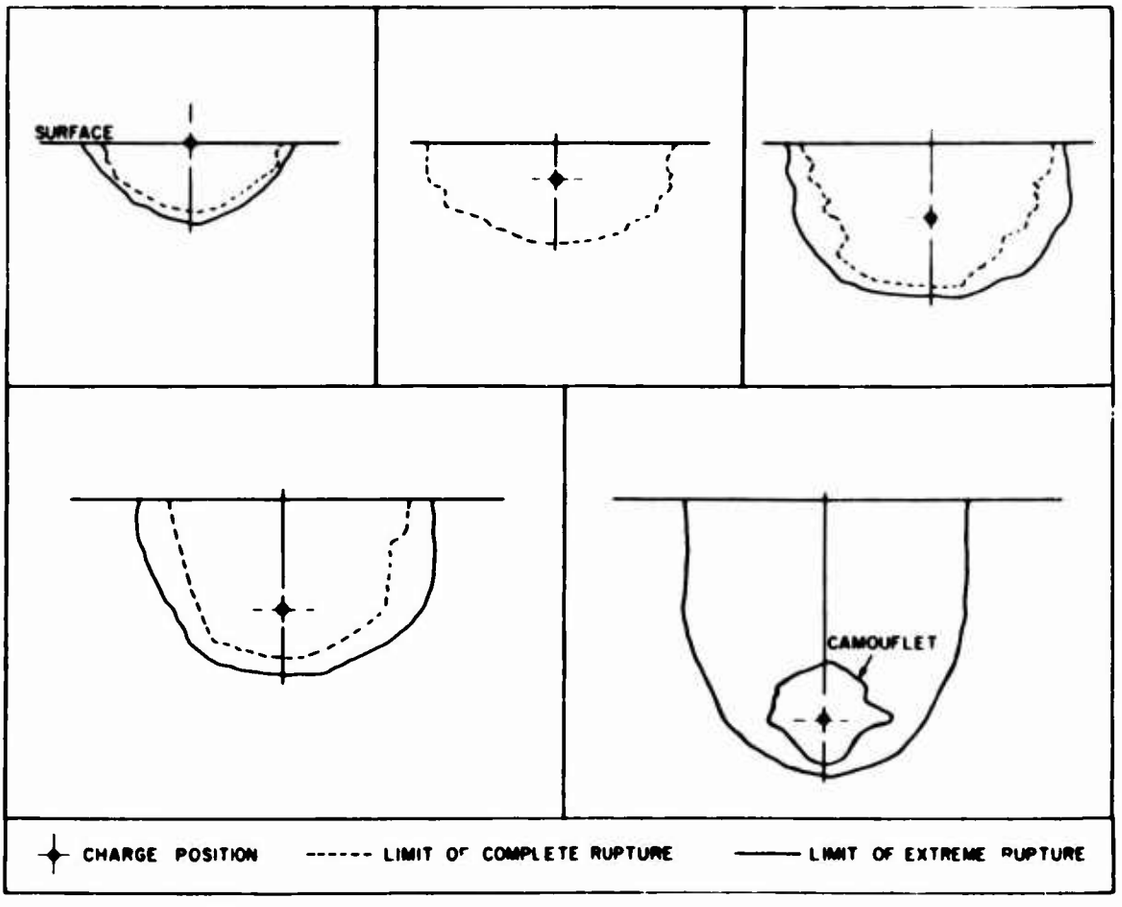

Figure 2. Crater limits for a series of shots fired at increasing depths below the snow surface (40-lb charges of composition explosive C-4). Some limits were not observed. (After Livingston, ref. 6)

exceed test scatter, and the writer has combined the data for all types of explosives without adjustment for this simple summary (Fig. 4-11).*

Much of the Livingston work is concerned with the effects of charge depth, and a dimensionless depth, termed the depth ratio Δ, is defined by dividing the actual charge depth by the critical charge depth. The critical depth is that charge depth below which the surface ceases to be fractured after firing, and it therefore corresponds roughly to the minimum depth for camouflet. Scaling by reference to the critical depth may later prove to have a broad significance for comparison of explosions in different ground materials, but for the present it seems necessary to provide working expressions for crater dimensions in dense snow using a charge yield scaling. To make the necessary conversion from the data, a relation between critical depth and charge weight is required. A suitable expression is

$$\Delta_* = 6.3\, W^{\frac{1}{3}} \qquad (2)$$

where Δ_* is critical depth (ft) and W is charge weight (lb). Equation 2 is plotted in

*For details of military explosives see ref. 13.

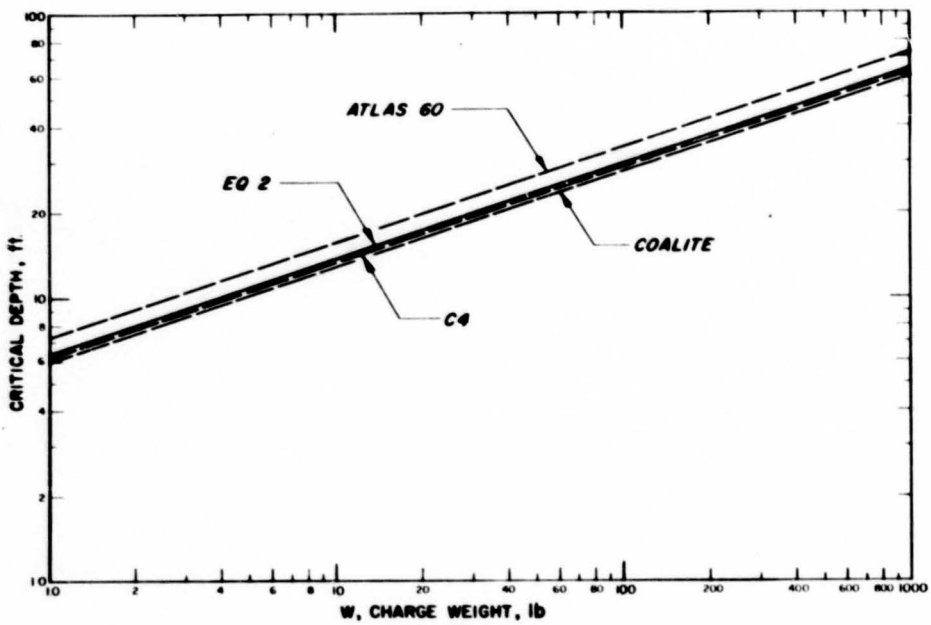

Figure 3. Critical charge depth and charge weight for several types of high explosive† fired in ice cap snow (max. charge 160 lb). (From data reported by Livingston, ref. 6)

Figure 3 for comparison with the scaling adopted by Livingston for individual explosives. Livingston apparently determined Δ_* empirically for a single charge weight, and then assumed cube root scaling.

Crater dimensions for surface shots on ice cap snow. The following approximate dimensions have been obtained by combining data for all types of explosives and also combining data for shots at the true surface with those for shots at the lower and denser surface formed by trench floors.†† The variations of both explosive type and snow type apparently gave effects which did not greatly exceed the limits of test scatter.

The radius of the apparent crater indicated by the data is

$$R_a = 0.35\,\Delta_* = 2.2\,W^{\frac{1}{3}} \qquad (3)$$

where the conversion from Δ_* to W is made from eq 2.

The depth of the apparent crater H_a varies somewhat:

$$H_a = 0.12\,\Delta_* \text{ to } 0.23\,\Delta_*$$

or $$H_a = 0.76\,W^{\frac{1}{3}} \text{ to } 1.4\,W^{\frac{1}{3}}.$$

The volume of the apparent crater V_a from direct observation and measurement is

† The commercial explosives used by Livingston were Atlas 60 (or A60) 60% gelatin dynamite, and Coalite 7S (or C7S), both manufactured by the Atlas Powder Co.

†† Some craters were made in an artificial snow surface, obtained by cutting broad trenches on the ice cap. This was done to utilize the natural density gradient, hence introducing snow density as a variable.

$$V_a \quad 5\,W \text{ to } 10\,W \tag{5}$$

and by calculation on the assumption of a paraboloid ($V = \frac{1}{2}\pi R^2 H$)

$$V_a \quad 5.8\,W \text{ to } 10.6\,W. \tag{6}$$

The dimensions of the complete rupture zone can be found from Figures 4 and 5.

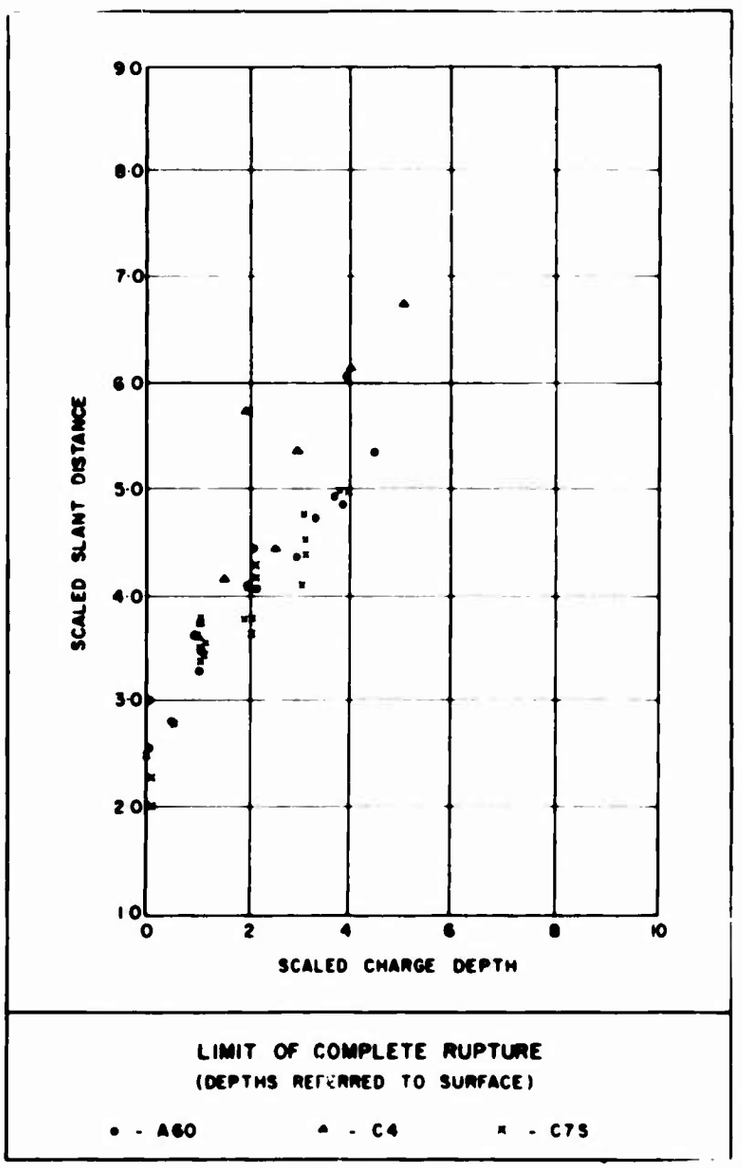

Figure 4. Scaled distance to the limit of complete rupture versus scaled charge depth (ft/lb$^{\frac{1}{3}}$). The points are for craters made by three different explosives (A60, C4, C7S) and depths are referred to the natural snow surface (at Site II on the Greenland Ice Cap). (After Livingston, ref. 6)

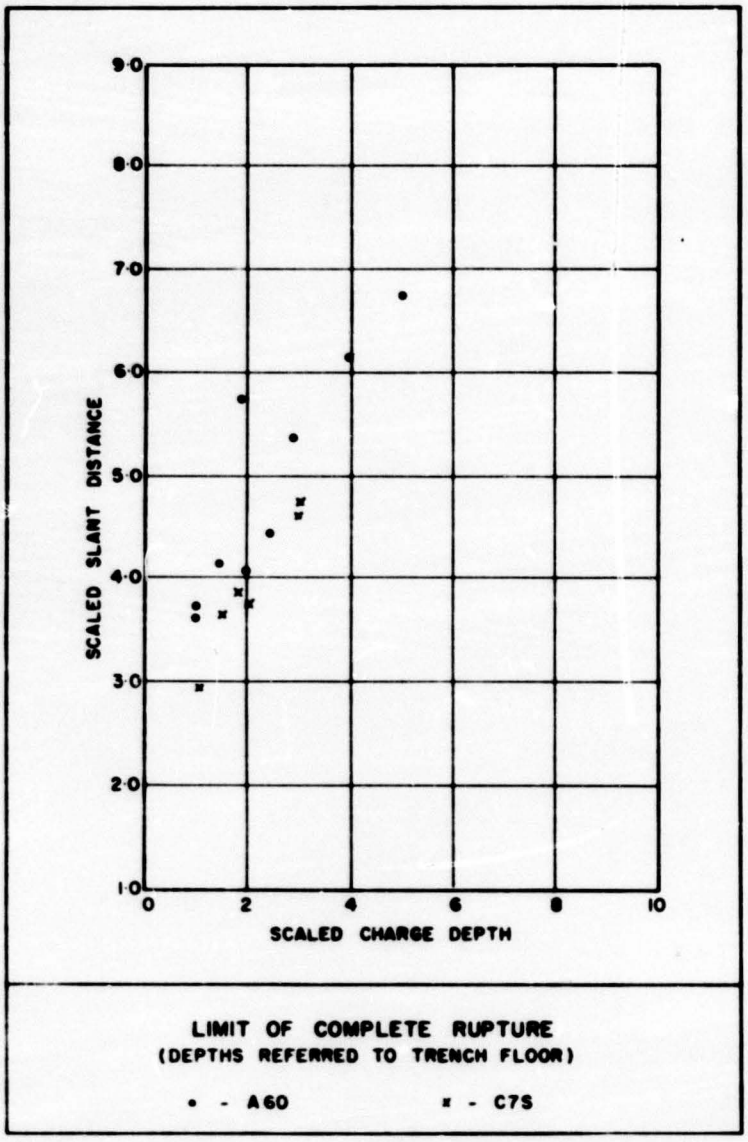

Figure 5. Scaled slant distance to the limit of complete rupture versus scaled charge depth ($ft/lb^{\frac{1}{3}}$). The explosions were in relatively dense snow, depths being referred to the bottom of a broad trench cut in the natural snowpack at Site II. (After Livingston, ref. 6)

They are:

Radius of complete rupture zone, $R_c = 2.5\ W^{\frac{1}{3}}$ (7)

Depth of complete rupture zone, $H_c = 0.3\Delta_* = 1.9\ W^{\frac{1}{3}}$. (8)

The radius to the extreme limit of rupture R_e is given by Figures 6 and 7, and is

$$R_e = 3.5\ W^{\frac{1}{3}}. \quad (9)$$

Crater dimensions for subsurface shots in ice cap snow. The following items refer to H. E. charges in the size range 2 - 160 lb. Extrapolation of the data to much higher ranges of yield is not recommended, since snow density increases with depth below the surface, and eventually the snow becomes hard impermeable ice, which has very different mechanical properties than the surface snow.

The radius of the apparent crater increases with charge depth up to a limit, then decreases again as the charge depth is further increased. The maximum radius of the apparent crater R_{am} occurs when the depth ratio is about 0.35, and its value is

$$R_{am} \approx 0.55\Delta_* \approx 3.5\, W^{\frac{1}{3}}. \qquad (10)$$

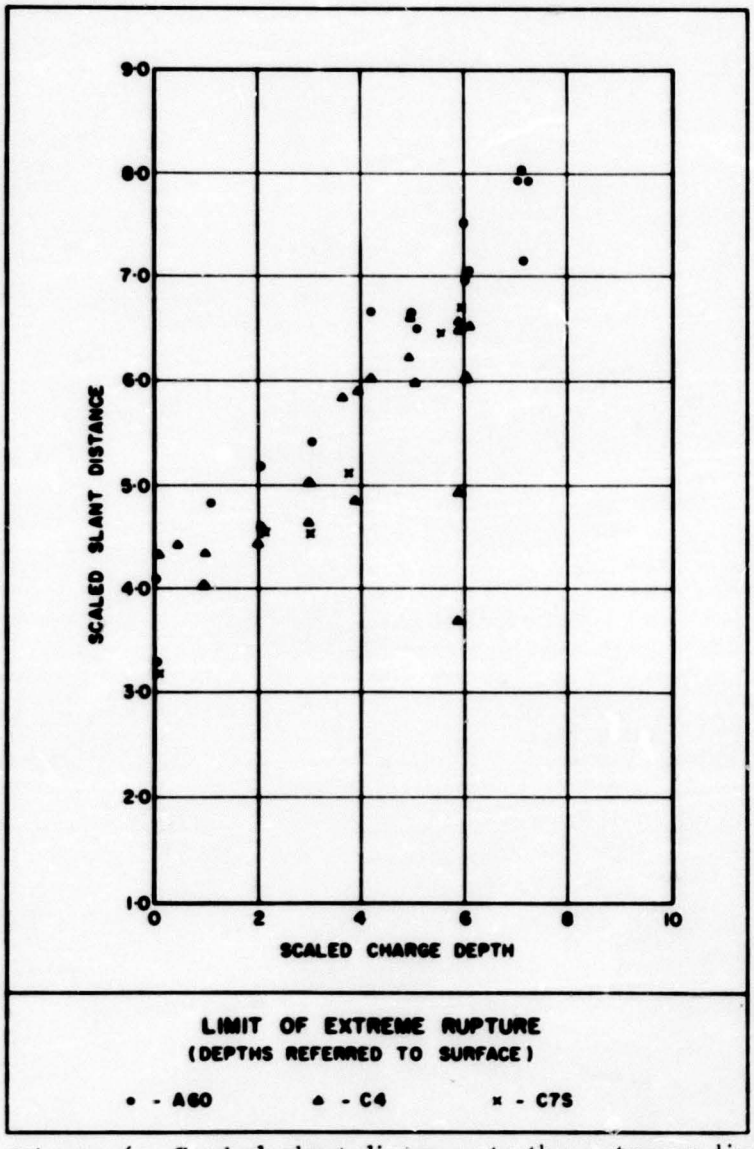

Figure 6. Scaled slant distance to the extreme limit of rupture versus scaled charge depth (ft/lb$^{\frac{1}{3}}$). Explosives used were A60, C4, and C7S. Depths are referred to the natural snow surface at Site II. (After Livingston, ref. 6)

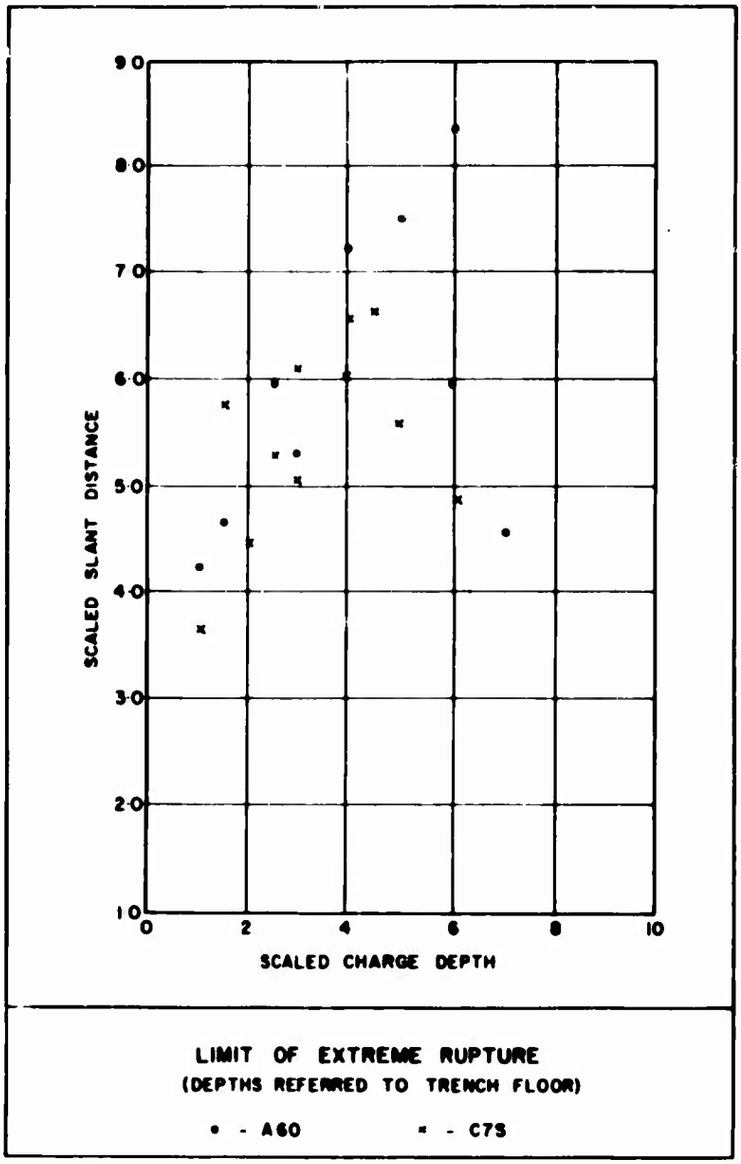

Figure 7. Scaled slant distance to the extreme limit of rupture versus scaled charge depth (ft/lb$^{\frac{1}{3}}$). Explosions in relatively dense snow with depths referred to the bottom of a broad trench cut in the natural snowpack at Site II. (After Livingston, ref. 6)

The depth of the apparent crater also rises to a maximum and then falls off again as charge depth is increased. The maximum crater depth H_{am} occurs when the depth ratio is about 0.15, and

$$H_{am} \approx 0.2\Delta_* \text{ to } 0.3\Delta_*$$

$$\text{or} \quad H_{am} \approx 1.3\,W^{\frac{1}{3}} \text{ to } 1.9\,W^{\frac{1}{3}}. \tag{11}$$

The maximum volume of the apparent crater occurs when the depth ratio is about 0.15, apparently because crater depth reaches a more pronounced maximum than crater radius. The maximum volume V_{am} found by direct measurement is

$$V_{am} \cdot 15\ W \text{ to } 35\ W \tag{12}$$

and the maximum volume found by calculation, using the paraboloid assumption and substituting radius and depth values for a depth ratio of 0.15, is

$$V_{am} \quad 24\ W \text{ to } 36\ W. \tag{13}$$

The radii of complete and extreme rupture (i.e. the distances measured on the surface from ground zero† to the appropriate limits) increase to a maximum and again decline as depth increases. Taking the data of Figures 4-7 and combining plots for surface and trench floor snow, linear relations between slant distance and charge depth seem to be indicated. (The slant distance is measured from the charge center to the intersection of the rupture limit with the surface.) Fitting straight lines to the data for complete rupture and extreme rupture, and converting these lines to plots of surface radius against charge depth by simple geometry, curves giving the charge depth for maximum rupture radius are obtained.

The maximum radius of complete rupture R_{cm} thus indicated occurs when charge depth is between $4\ W^{\frac{1}{3}}$ and $6\ W^{\frac{1}{3}}$, and is

$$R_{cm} \approx 4.1\ W^{\frac{1}{3}}. \tag{14}$$

The maximum radius of extreme rupture R_{em} seems to occur between charge depths of $3\ W^{\frac{1}{3}}$ and $5\ W^{\frac{1}{3}}$, and has a value

$$R_{em} \approx 4.6\ W^{\frac{1}{3}}. \tag{15}$$

It might be noted that the slant distances plotted in Figures 4-7 become insensitive indicators at large charge depths for obvious geometrical reasons. In fact, straight lines fitted to the data appear to violate the definitions of complete and extreme rupture limits at large charge depths.

The complete rupture depth is defined as the vertical distance from surface level to the limit of complete rupture at the center of the crater. It is thus the sum of the charge depth and the vertical distance from the charge to the limit of complete rupture and, keeping this in mind, Figures 8 and 9 nicely demonstrate that the limit of complete rupture stays a constant distance beneath the charge (a straight line with a slope of unity gives a good fit to the data). This distance from the charge to the bottom of the complete rupture zone is about $0.28\Delta_*$, or $1.8\ W^{\frac{1}{3}}$.

Volume enclosed by the limit of complete rupture. The data giving volumes enclosed by the limits of complete rupture are in the form of an "energy utilization number," which is plotted against depth ratio (Fig. 10, 11). The energy utilization number is defined as the volume within the limits of complete rupture divided by the corresponding volume for optimum charge depth, where optimum charge depth is that depth of burial which leads to breakage of maximum volume of material for a given charge.

In conformance with the above definition, energy utilization number must rise to a maximum value of unity at the optimum depth and thereafter decline again as charge depth is further increased. In a homogeneous material the energy utilization number will remain constant for all depths below the critical depth. The data do not appear to

---

†Ground zero: A point on the surface immediately beneath, or above, the center of the explosion.

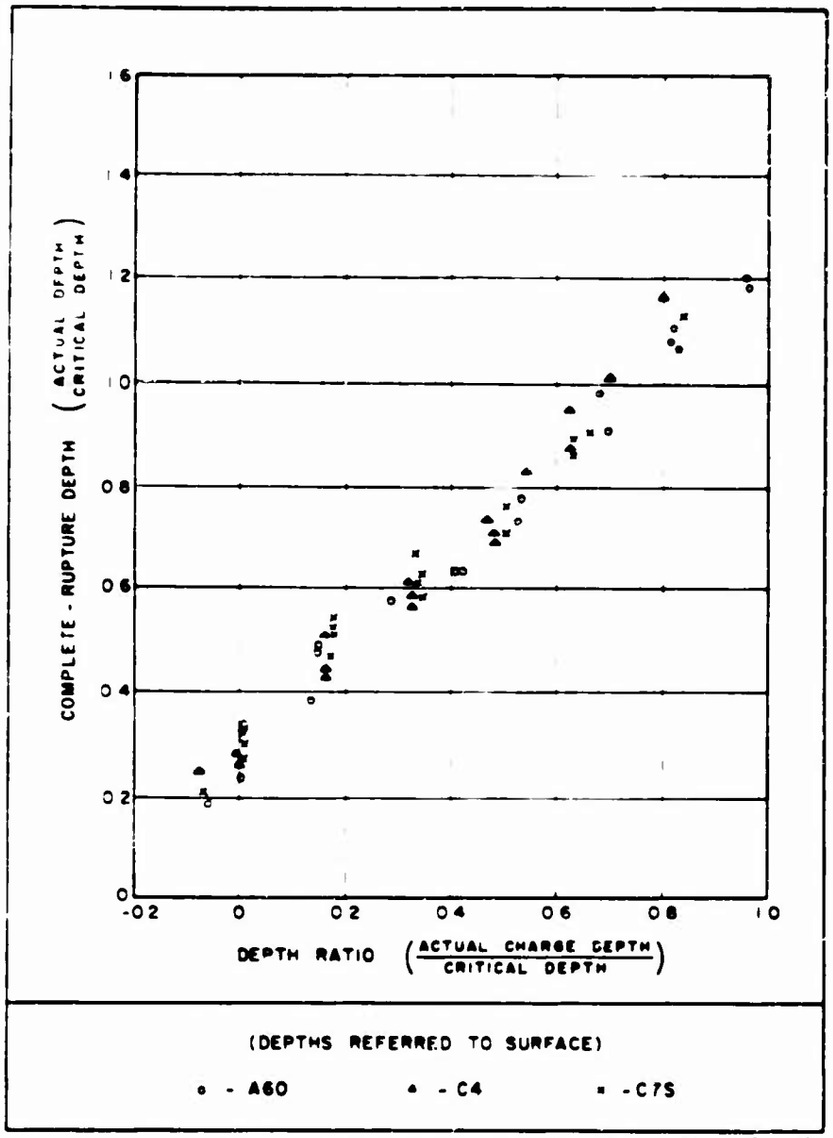

Figure 8. Scaled complete-rupture depth versus depth ratio. Depths are referred to the natural snow surface. (Depth ratio is actual depth divided by critical depth.) (After Livingston, ref. 6)

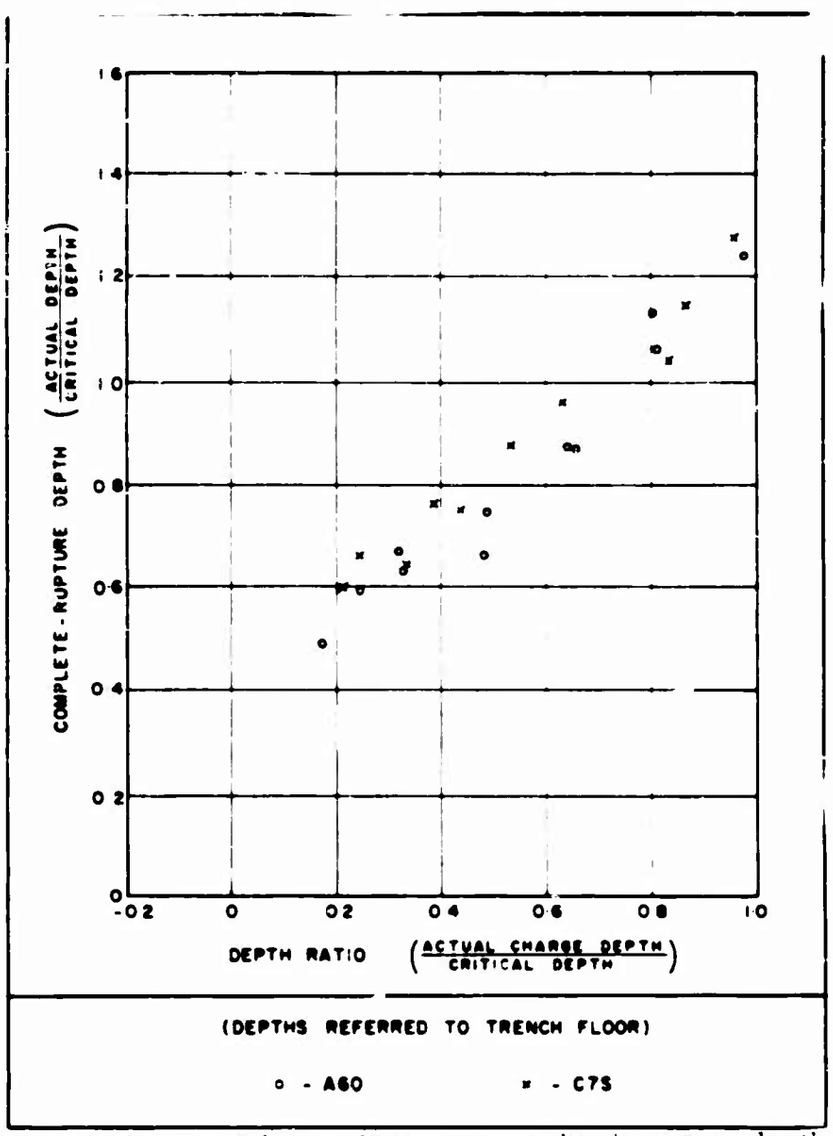

Figure 9. Scaled complete-rupture depth versus depth ratio for explosions in relatively dense snow beneath the floor of a broad trench cut through the natural snowpack. (After Livingston, ref. 6)

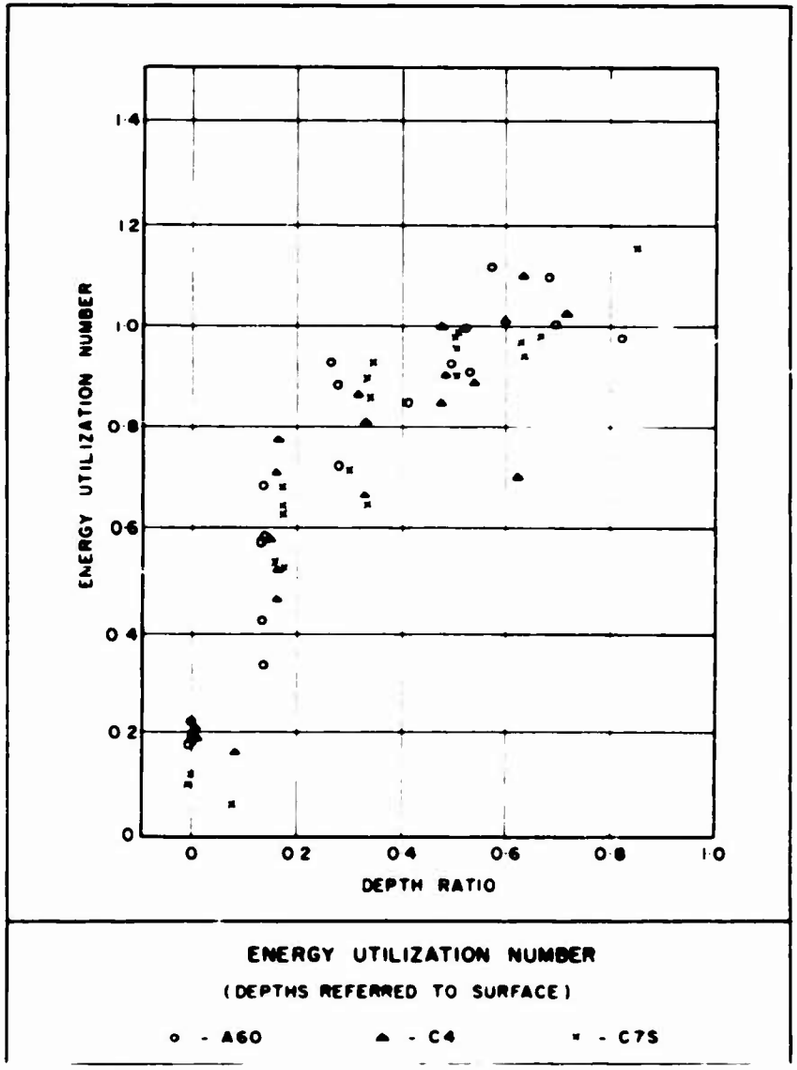

Figure 10. Energy utilization number versus depth ratio. Depths referred to the natural snow surface. (After Livingston, ref. 6)

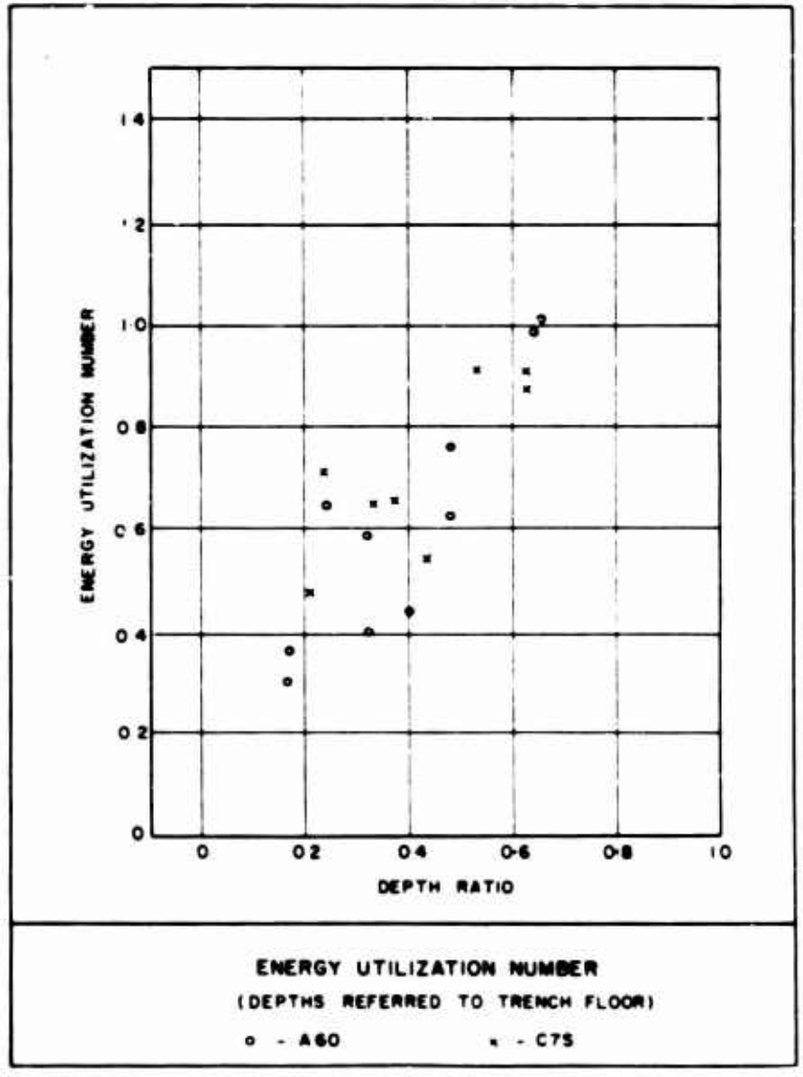

Figure 11. Energy utilization number versus depth ratio. Depths referred to the bottom of a broad trench cut in the natural snowpack. (After Livingston, ref. 6)

define a maximum, but Livingston gives the optimum depth for surface snow as approximately $0.58\Delta_*$ ($3.65\ W^{\frac{1}{3}}$), and for denser trench snow as approximately $0.67\Delta_*$ ($4.22\ W^{\frac{1}{3}}$).

To provide information on absolute volumes for the zone of complete rupture, volume per unit charge weight has been plotted against scaled charge depth for surface snow and trench snow in Figures 12 and 13. It should be remembered that linear extrapolation from these data is not permissible; a constant volume should be reached as depth increases past the critical depth. As yet there is little evidence of a decline in volume when the optimum depths given by Livingston are exceeded.

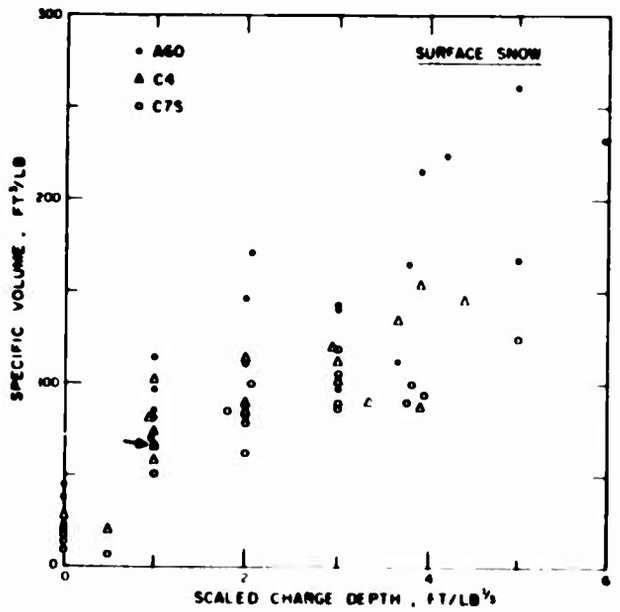

Figure 12. Volume enclosed by the limit of complete rupture per unit charge weight plotted against scaled charge depth for three types of explosive in surface snow on the Greenland Ice Cap. Arrow indicates one C4 and five C7S plots. (From Livingston's data, ref. 6)

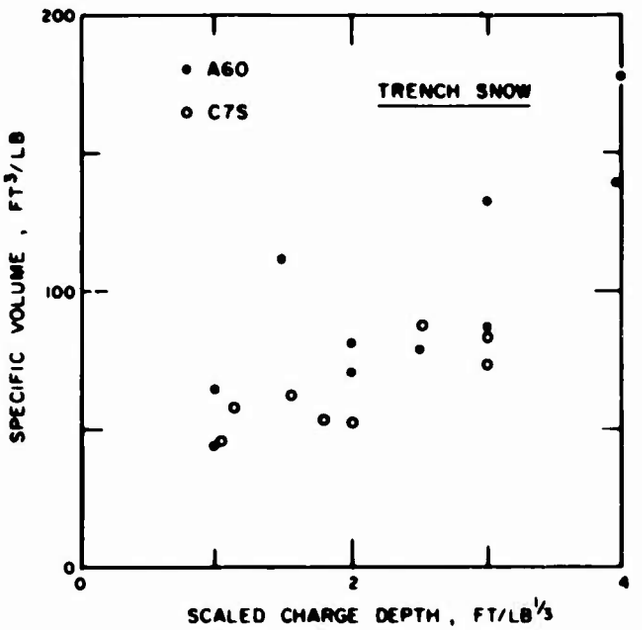

Figure 13. Volume enclosed by the limit of complete rupture per unit charge weight plotted against scaled charge depth. The depths are referred to the base of a broad trench cut in the natural snowpack. (From Livingston's data, ref. 6)

The foregoing data on crater dimensions are summarized in Tables I, II and III.

Ground shock

The rapid expansion of gases in an undersnow explosion induces shock waves in both the ice and air components of the snow. The fraction of the total energy expended on ground shock varies with the depth of burial, ranging from a small proportion for surface bursts to virtually 100% for a camouflet. Some of the energy in an air blast is converted to ground shock when the air wave strikes the surface.

Figures 14 and 15 give some representative records of undersnow pressure at various distances from small subsurface explosions on the Greenland Ice Cap. Very close to the explosion, pressure rise at the undersnow shock front is abrupt and the decay from peak overpressure is of an exponential form (see the record for shot no. 211, gage position 1). Further away from the explosion, pressure rise becomes more gradual and there is no sharply defined peak pressure. The decay of overpressure is relatively slow, giving a long positive phase.

Table I. Crater dimensions for surface shots on ice cap snow. (Author's interpretation of Livingston's data[6])

Limit	Radius (ft)	Depth (ft)	Volume (ft^3)
Apparent crater	$2.2\ W^{\frac{1}{3}}$	$0.76\ W^{\frac{1}{3}} - 1.1\ W^{\frac{1}{3}}$	$5\ W - 10\ W$
Complete rupture zone	$2.5\ W^{\frac{1}{3}}$	$1.9\ W^{\frac{1}{3}}$	—
Extreme rupture zone	$3.5\ W^{\frac{1}{3}}$	—	—

W charge weight (yield) in lb.

Table II. Crater dimensions for subsurface shots in ice cap snow. (Author's interpretation of Livingston's data[6])

Limit	Maximum radius		Maximum depth		Maximum volume	
	R_m (ft)	Charge depth (ft)	H_m (ft)	Charge depth (ft)	V_m (ft^3)	Charge depth (ft)
Apparent crater	$3.5\ W^{\frac{1}{3}}$	$2.2\ W^{\frac{1}{3}}$	$1.3\ W^{\frac{1}{3}} - 1.9\ W^{\frac{1}{3}}$	$0.945\ W^{\frac{1}{3}}$	$15\ W - 35\ W$	$0.945\ W^{\frac{1}{3}}$
Complete rupture zone	$4.1\ W^{\frac{1}{3}}$	$4\ W^{\frac{1}{3}} - 6\ W^{\frac{1}{3}}$	--	—	—	—
Extreme rupture zone	$4.6\ W^{\frac{1}{3}}$	$3\ W^{\frac{1}{3}} - 5\ W^{\frac{1}{3}}$	—	—	—	—

W charge weight (yield) in lb.

Table III. Approximate dimensions of apparent crater for shots in seasonal snow (see ref. 1, 17 and 23).

Surface shots		Subsurface shots	
Radius, R_a (ft)	Depth, H_a (ft)	Maximum radius, R_{am_1} (ft) (Charge depth $\approx 1.3\ W^{\frac{1}{3}}$ ft)	Maximum depth, H_{am_1} (ft) (Charge depth $\approx 1.3\ W^{\frac{1}{3}}$ ft)
$2.8\ W^{\frac{1}{3}}$	$1.8\ W^{\frac{1}{3}}$	$3.2\ W^{\frac{1}{3}}$	$2.0\ W^{\frac{1}{3}}$

The propagation of shock through the ice and air components of the snow may take two different forms, although intimate interaction between the two components probably precludes a strong distinction. Figure 16 gives the results of an experiment in which measurements of air pressure in a small cavity were compared with pressure measurements in the general snow mass at the same position. Pressure rise appears to be more gradual in the interstitial air than in the general mass, and the peak pressure is more clearly defined.

Figure 17 gives typical records from undersnow accelerometers placed at a scaled slant distance of 4 $lb/ft^{\frac{1}{3}}$ from explosions fired at two different depths.

Snow has strong attenuating properties in comparison with common rocks and soils, and waves traveling out from a subsurface explosion in snow are rapidly damped. In Figure 18 peak overpressure has been plotted against scaled slant distance from the explosion to give an attenuation relationship for ice cap snow. On the same graph a corresponding plot has been made for dense glacier ice. Both plots summarize measurements made in Greenland by USA SIPRE and Waterways Experiment Station.[4] A comparison with attenuation in seasonal snow[17] is also shown.

At any given scaled distance from the explosion, overpressure is much smaller in snow than in ice. At a scaled distance of 1 $ft/lb^{\frac{1}{3}}$ the overpressure in ice is about one

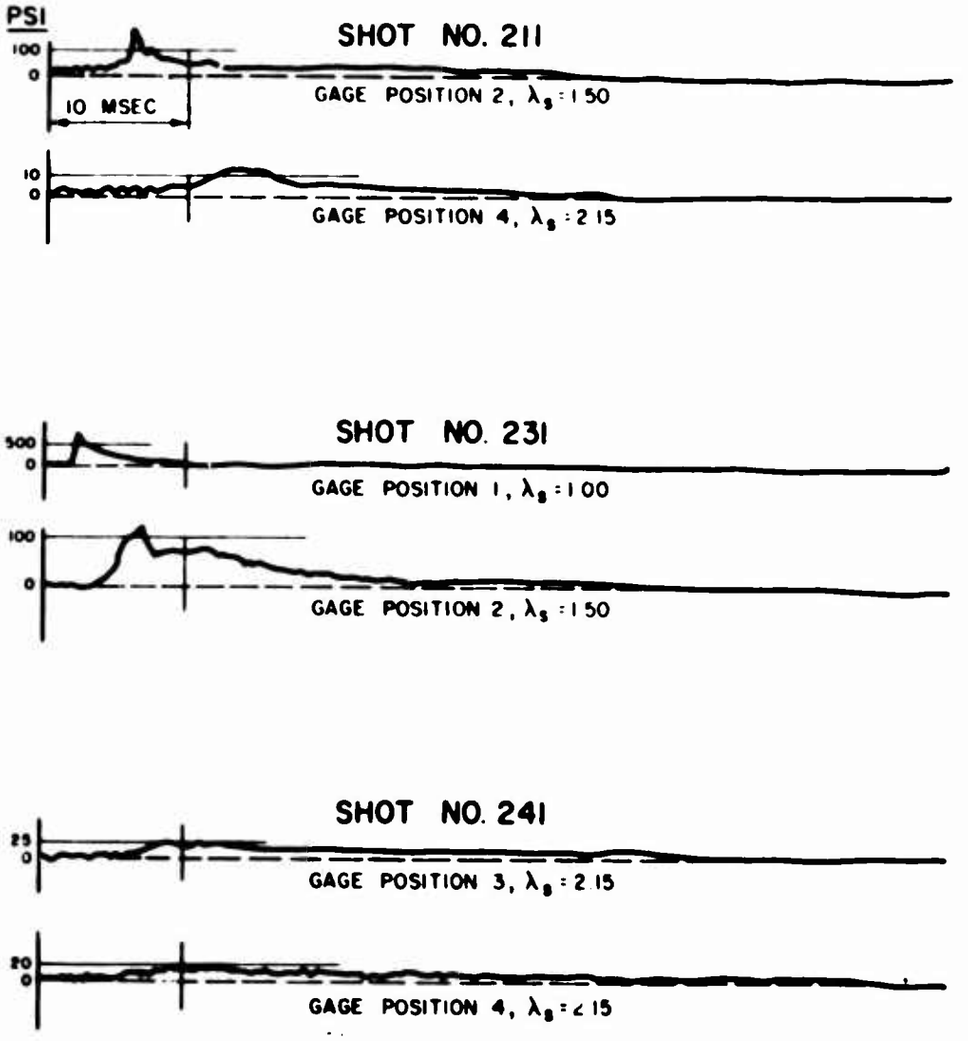

Figure 14. Representative records of undersnow pressure taken by piezoelectric gages. The symbol λ denotes a scaled distance in $ft/lb^{\frac{1}{3}}$. (After Ingram and Halper, ref. 4)

order of magnitude higher than in snow, while at a scaled distance of 10 $ft/lb^{\frac{1}{3}}$ the overpressure in ice is more than two orders of magnitude higher than in snow. The superior coupling of energy to the ice is largely due to closer match of the mechanical impedance between explosive and ice.

In Figure 18 the attenuation curve for air is also shown (actually it is a curve for air overpressures at the snow surface rather than for free air). An interesting point is that snow attenuates a shock more rapidly than either of its two component materials alone. We note that for snow and its component materials (ice and air) an inverse cube relationship, while not exact, provides a fair approximation for the decay of overpressure with distance in the range shown.

In ice caps snow density increases with depth, so that finally the snow becomes ice in the deeper layers. Thus the elastic properties, and hence the speed of wave propagation, increase with depth. The result is that waves are refracted, and in the surface snow some distance from an explosion there is disturbance from waves which travel directly through the surface layers and also from waves refracted from the deep layers. In some positions disturbance due to the waves refracted from deep ice may conceivably be more severe than that due to the more direct waves, so that refraction becomes a consideration when "safe distances" for structures are to be decided. Actually the strong "late-arrival" accelerations observed during tests on the Greenland Ice Cap are probably due to sudden arrest of the snow after passage of the ground wave.[4]

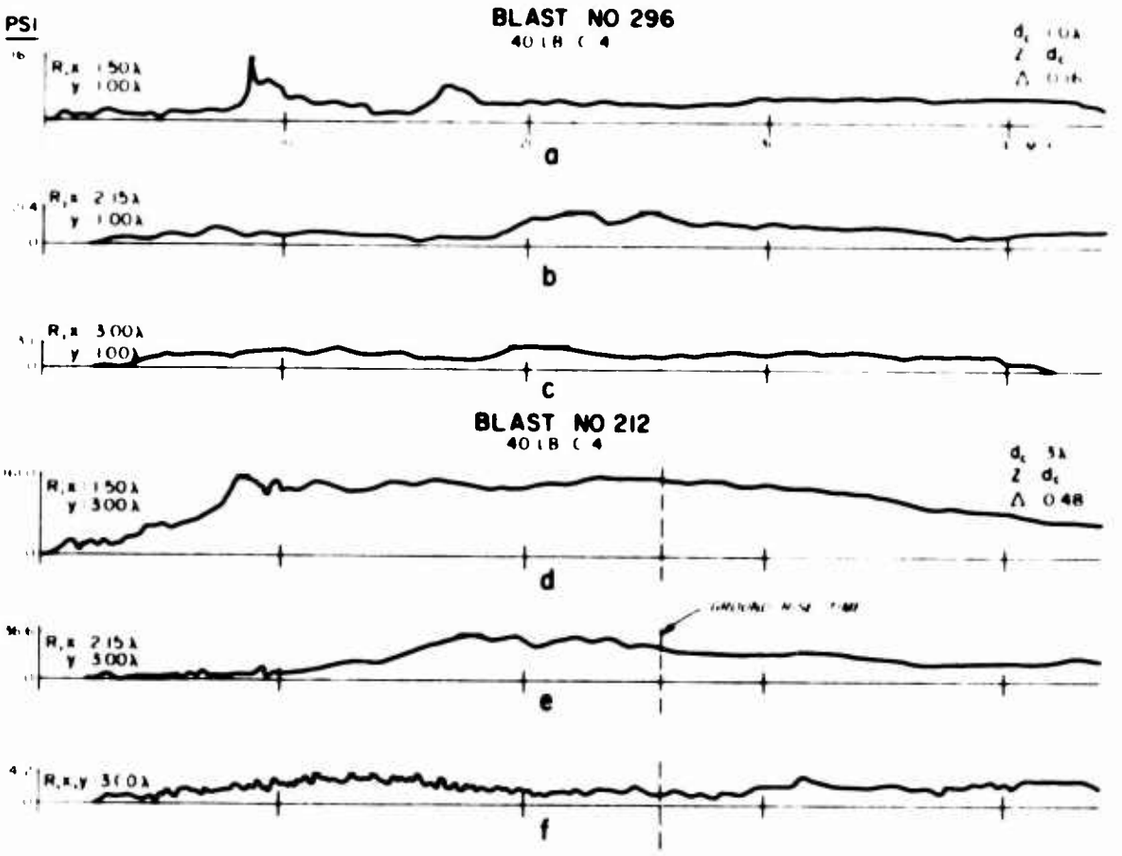

Figure 15. Typical records of undersnow shock at various distances from the blast. In shot 296 the charge was 1 ft/lb^{1} beneath the surface, and in shot 212 it was at a depth of 3 ft/lb^{1}. In each case the gages were at the same depth as the charge. Records (a) and (d) are taken 1.5 ft/lb^{1} from the shot, (b) and (e) at 2.15 ft/lb^{1}, and (c) and (f) at 3.0 ft/lb^{1}. (After Livingston, ref. 6)

Response of snow to intense compressive loading

When a mass of snow is subjected to a high-speed compressive loading by an explosion, the snow particles are set in motion as the mass is traversed by an elastic dilatational wave and a "plastic" compression wave.[21] By considering conservation of mass and momentum across the wave fronts, the so-called Rankine-Hugoniot equations can be derived (the derivation was originally for shock fronts in a compressible fluid). The relations are:

Across the elastic wave front	p_1	$\gamma_0 v_0 u_1$
	γ_1	$\gamma_0 v_0 / (v_0 - u_1)$
Across the plastic wave front	p_2	$p_1 + \gamma_1 (U - u_1)(u_2 - u_1)$
	γ_2	$\gamma_1 (U - u_1)/(U - u_2)$

where p is pressure normal to the wave front, v_0 is elastic wave velocity in undisturbed snow (see next section), u is snow particle velocity, U is velocity of propagation of plastic wave, and γ is snow density. Subscripts 1 and 2 refer to conditions ahead of and immediately behind the wave front respectively.

Values of v_0, u and U have been determined from one-dimensional experiments on coherent snow.[21] A snow sample was set on a steel anvil and compressed at high speed by a hammer driven explosively against it. Displacements of reference marks on the

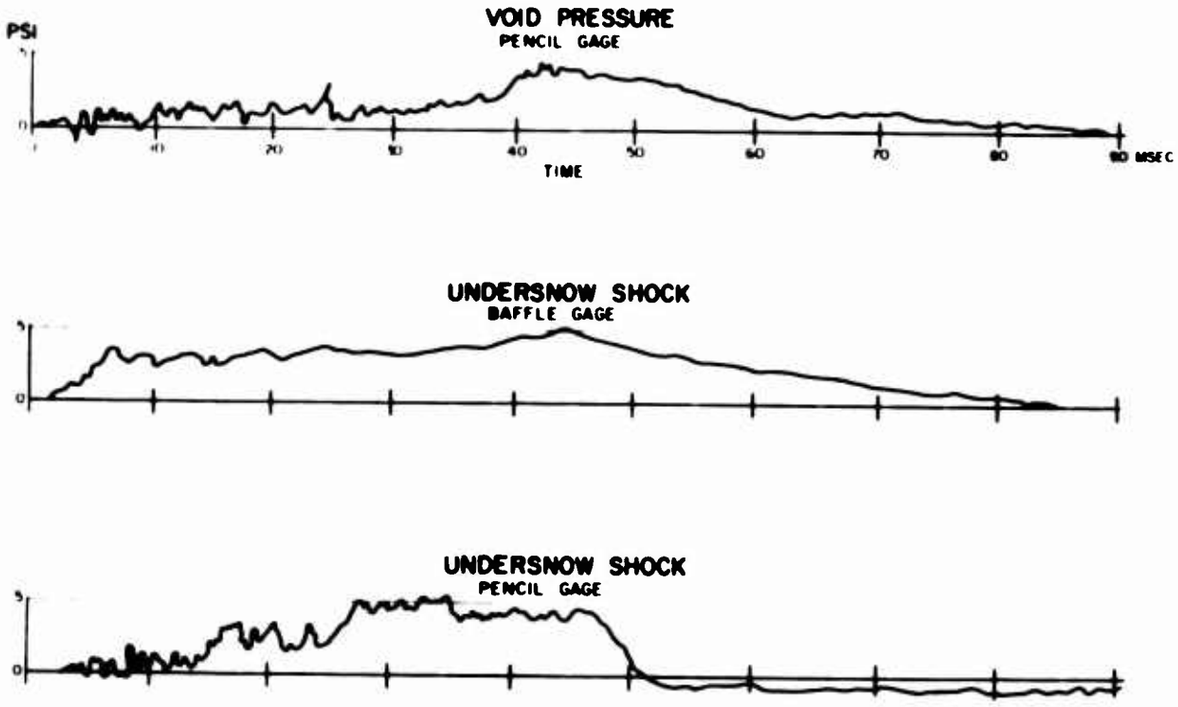

Figure 16. Simultaneous records of gross undersnow shock and air shock in a small cavity in the snow. Gages were 4 ft/lb$^{\frac{1}{3}}$ from the shot; gages and charge at a depth of 2 ft/lb$^{\frac{1}{3}}$. (After Livingston, ref 6) [Note: specialists of USAEWES question the validity of pencil gage measurements in the snow.]

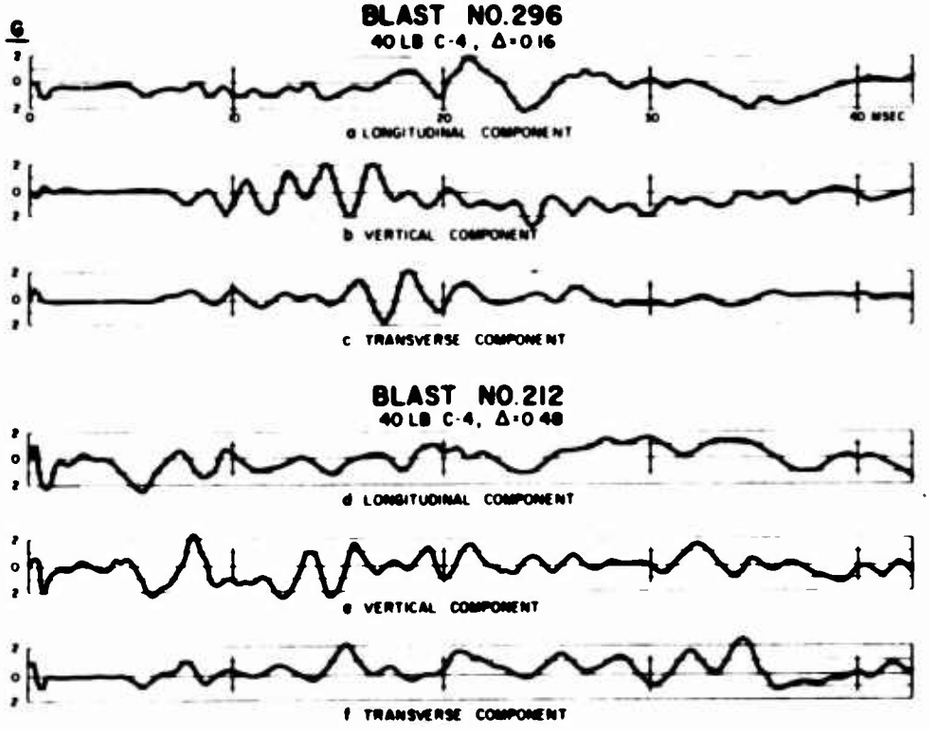

Figure 17. Records from undersnow accelerometers for two blasts (see Fig. 15). Slant distance to each accelerometer is 4 ft/lb$^{\frac{1}{3}}$; accelerometer was 1 ft/lb$^{\frac{1}{3}}$ (shot 296) and 1.5 ft/lb$^{\frac{1}{3}}$ (shot 212) below surface. (After Livingston, ref. 6). [Note: specialists at USAEWES caution that high-frequency components in these traces may have been caused by vibration of accelerometer canisters, which were not matched to the density of the snow displaced.]

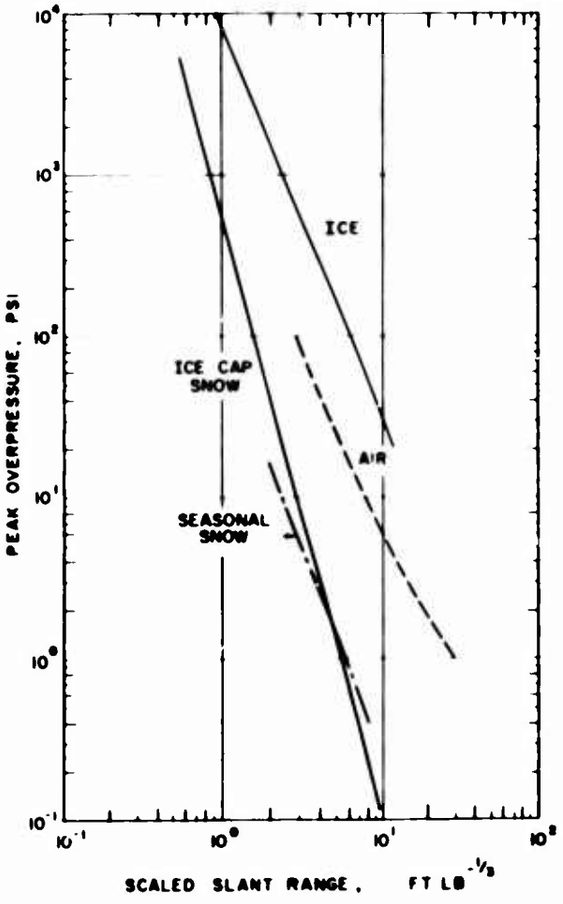

Figure 18. Decay of peak overpressure with distance in snow, ice, and air. (Snow and ice data summarized from ref. 4 and 17, air curve from Figure 29)

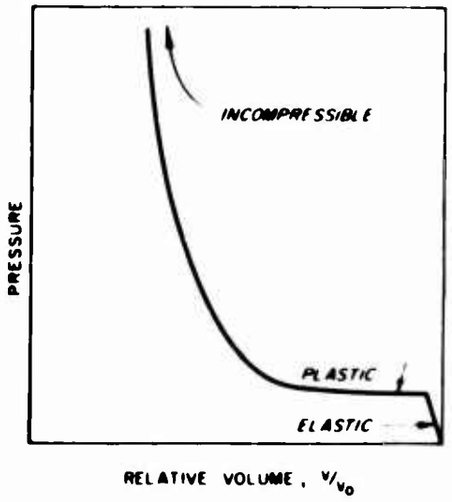

Figure 19. Idealized relationship between pressure and volume (Hugoniot curve) for an explosively loaded material which is capable of sustaining elastic and plastic waves.

snow were recorded on a streak camera. The resulting values may be substituted into the above equations to give what is known as the Hugoniot equation of state for the snow; the graphical presentation is called the Hugoniot curve.

The Hugoniot curve relates pressure and specific volume (volume relative to initial volume), and is essentially a stress/strain relation. In its general form for a material which supports both elastic and plastic waves, the curve exhibits elastic strain up to a certain yield stress, plastic compression, and finally an approach to the incompressible state (Fig. 19). In Figure 20 some examples of Hugoniot curves for ice cap snow from Greenland are shown.

Elastic waves in snow

Beyond the extreme limit of rupture an explosive disturbance becomes attenuated and slowed to the extent that it ceases to be a true shock wave; outside this radius it travels at the speed of sound and the snow is capable of responding elastically to its passage. The energy used for elastic wave propagation is that remaining after expenditure of energy on fracturing, displacing and deforming in the crater region. The elastic waves travel outwards in a spherical pattern in isotropic snow, becoming reduced in intensity as a result of spreading over an ever-increasing area and also as a result of viscous absorption of energy by the snow.

The principal elastic waves affecting snow are: (1) longitudinal waves (compression waves, P-waves), (2) transverse waves (shear waves, S-waves), (3) surface waves (Rayleigh and Love waves). The speeds of longitudinal and transverse waves can be related to the dynamic elastic constants of snow by the following expressions:

$$\text{Longitudinal - } v_p = \left[\frac{E}{\gamma}\,\frac{(1-\nu)}{(1-2\nu)(1+\nu)}\right]^{\frac{1}{2}} \qquad (16)$$

$$\text{Transverse - } v_s = \left[\frac{E}{\gamma}\,\frac{1}{2(1+\nu)}\right]^{\frac{1}{2}} \qquad (17)$$

where E is Young's modulus (in dynes/cm^2), ν is Poisson's ratio, and γ is snow density (in g/cm^3). The Rayleigh surface wave is sometimes called "ground roll"; close to a large explosion it may be felt as an oscillation of the surface.

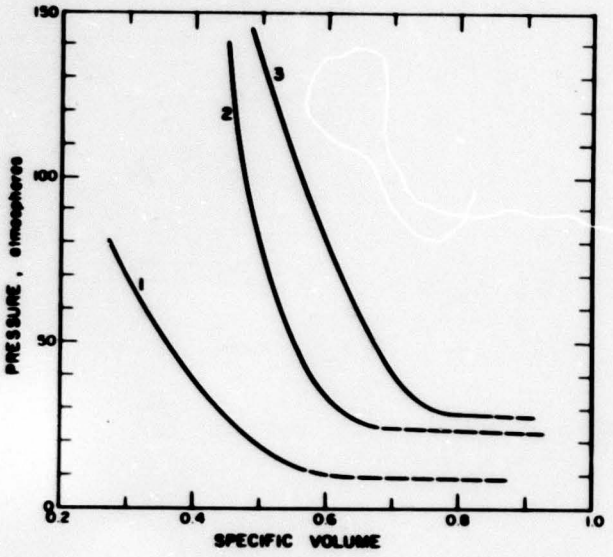

Figure 20. Samples of Hugoniot relations calculated from wave velocity measurements on ice cap snow subjected to compressive loading by explosives. Curve 1, $\gamma_0 = 0.39$ g/cm^3. Curve 2, $\gamma_0 = 0.53$ g/cm^3 (snow stratification normal to direction of wave travel). Curve 3, $\gamma_0 = 0.53$ g/cm^3 (snow stratification parallel to direction of wave travel). (From Napadensky, ref. 21)

In isotropic snow, the energy of a wave, which is proportional to the square of the amplitude, is inversely proportional to the square of the distance from the source because of spherical spreading, and therefore amplitude must be inversely proportional to the distance from the source. The absorption of energy due to internal dissipation in the snow should result in an exponential decrease of amplitude with distance traveled so that the expression giving the combined attenuation effects of spreading and absorption will be of the form

$$A = A_0 \frac{e^{-\alpha r}}{r} \qquad (18)$$

where A is wave amplitude at radius r from the source

A_0 is initial amplitude of the elastic wave

α is an attenuation constant.

No specific data on α have been found, but its broad characteristics may be surmised from experiments such as those made by Nakaya[8] with the viscoelastic meter. α will vary with frequency and with snow type, and there will be a tendency for high frequency components to be lost more rapidly than those of lower frequencies because of selective energy absorption by viscosity, internal friction and scattering.

Elastic wave velocity in snow depends on density and grain structure and, to a small extent, temperature. Data summarized elsewhere[7] show P-wave velocity increasing from about 700 m/sec in snow of density 0.3 g/cm^3 to about 3400 m/sec in snow of density 0.8 g/cm^3, the snow being well bonded in each case. Since natural ice cap snows increase in density with depth below the surface, velocity increases with depth and waves are refracted. In snow undergoing the metamorphic process termed age-hardening, wave velocity increases with time as intergranular bonds form between the ice grains. Temperature change appears to have only a slight effect, judging from experiments on ice and from the temperature-dependence of Young's modulus for snow.

In dense snow a temperature drop of one degree C probably increases wave speed by something of the order of 0.1%. Further information on elastic properties of snow is given in Part III, Section A1 of this series.

Elastic waves obey the laws of reflection and refraction established for electromagnetic waves, and the principles of reflection and refraction are applied in geophysical investigation on ice caps. Details are given in Part II, Section A2, Exploration geophysics.

Blast waves in air

When an explosion occurs at or above the surface a shock wave travels radially outwards through the air, spherical wave fronts being reflected from the surface. Initially the shock wave has a very high velocity, in excess of the speed of sound, but as it progresses it weakens and slows down; eventually the blast wave travels at the speed of sound, thus ceasing to be a true shock wave.

In an air blast, pressure is highest at the moving shock front, where there is an abrupt rise from ambient air pressure. Behind the shock front pressure falls off gradually. The excess of pressure above original ambient air pressure is called the overpressure. As the blast wave travels outwards from its source, pressure at the moving front steadily decreases and pressures behind the front also decline. At a certain distance from the explosion, pressure behind the front drops below normal atmospheric pressure, giving a "negative phase." Figure 21 shows schematically successive stages in the outward progression of a blast wave, while Figure 22 gives the variation of overpressure with time at a fixed location and illustrates the meaning of "positive phase" and "negative phase." It is the change from positive to negative overpressure which is responsible for the reversal of displacement experienced during passage of a blast wave.

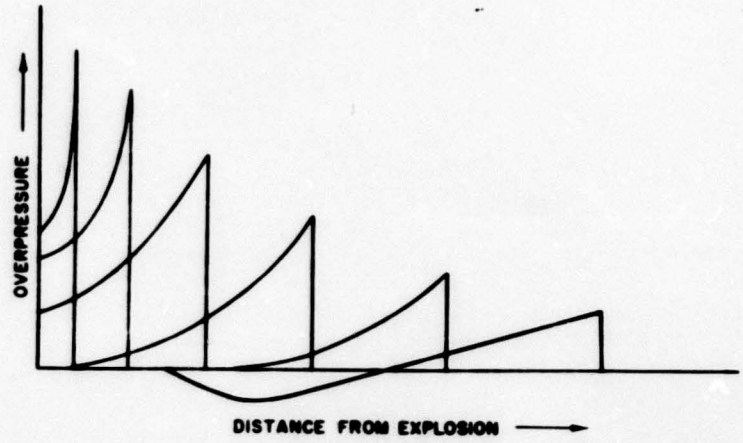

Figure 21. Diagram showing successive stages in the outward movement of a blast wave in air. The parameter is time, so that the curves are relationships between overpressure and distance at successive instants.

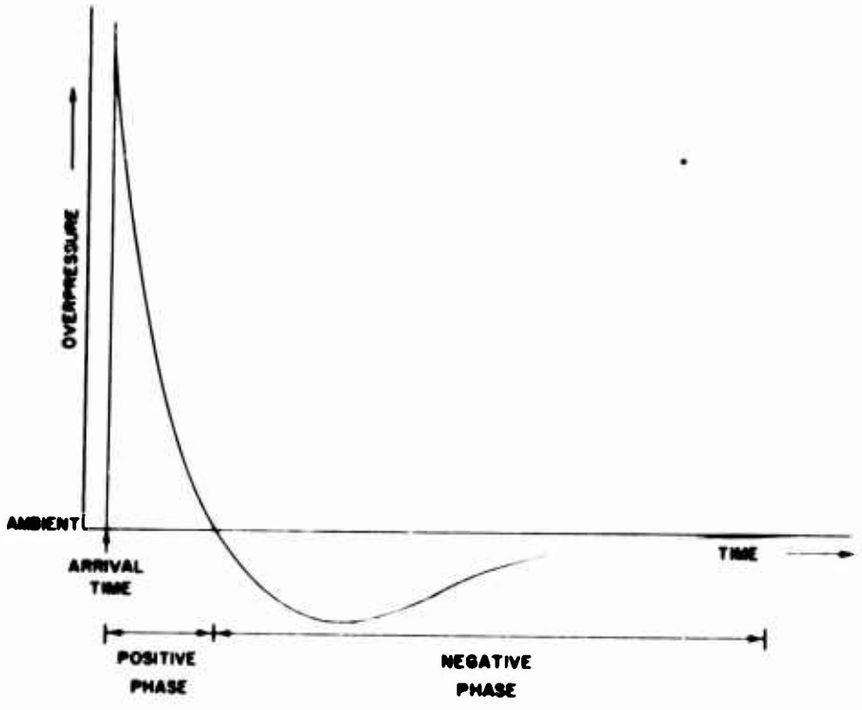

Figure 22. Simplified diagram showing the variation of air blast overpressure with time at a fixed location(sufficiently distant from ground zero for a negative phase to have developed).

Surface reflection of blast waves. The shock wave from an air blast is reflected when it strikes the ground or snow surface. Close to ground zero regular reflection occurs and the incident and reflected waves do not merge above the surface (providing the burst is high enough). Thus, in the region of regular reflection, two shocks are felt at a point above the surface — one resulting from the incident, or direct, wave overpressure and a second being total overpressure after reinforcement by the reflected shock.

Further away from ground zero the reflected wave is able to travel appreciably faster than the incident wave, since the air through which it passes has been heated by adiabatic compression during passage of the initial shock. The reflected wave can therefore catch up with the incident wave and fuse with it to form a single shock front, which is termed a Mach front. This is called Mach, or irregular, reflection. Figure 23 gives a schematic representation of wave fusion and the outward progression of a Mach front. The point at which incident and reflected waves unite to form a Mach front is called the triple point, and the fused shock wave beneath this point is known as the Mach stem.

In Figure 24 the scaled height of the triple point, or Mach stem height, is plotted against scaled horizontal distance from ground zero for four different heights of burst over ice cap snow. The curves are thus triple-point loci.

When a blast wave strikes a reflecting surface it is reflected with overpressures higher than those of the incident wave. For normal incidence on a rigid reflecting surface, the reflected pressure can be calculated if the incident overpressure, the initial ambient air pressure, and the ratio of specific heats are known. In Figure 25 the theoretical reflected pressure for a rigid surface (which apparently corresponds fairly well with observations for reflection from most natural solid surfaces) is compared with observed reflected pressure for normal incidence on a natural ice cap snow surface. The reflected pressures from snow are about 30% lower than those from a rigid surface in the range observed.

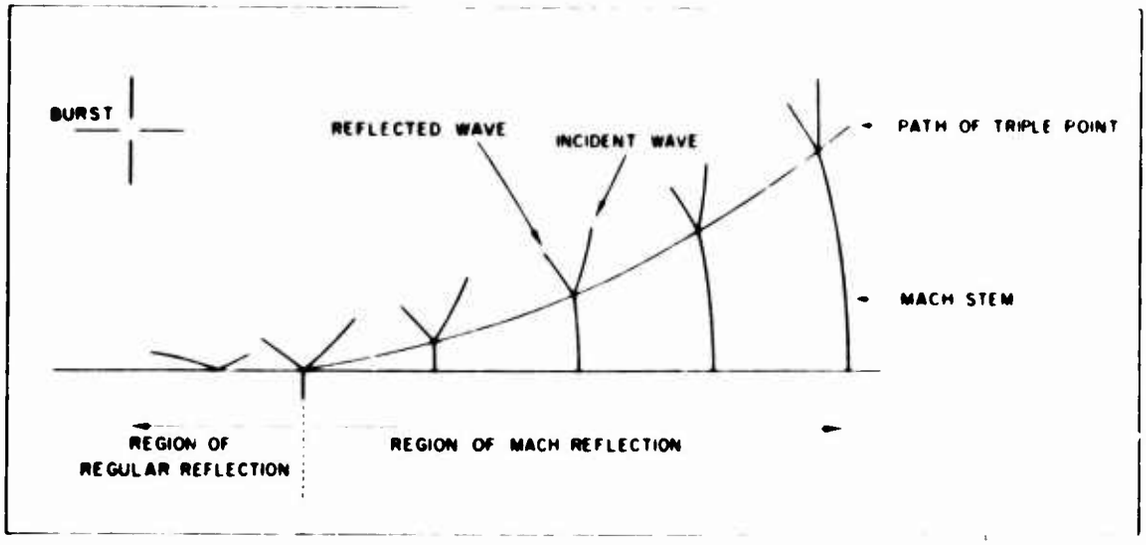

Figure 23. Diagram illustrating wave fusion and the outward progression of a Mach front.

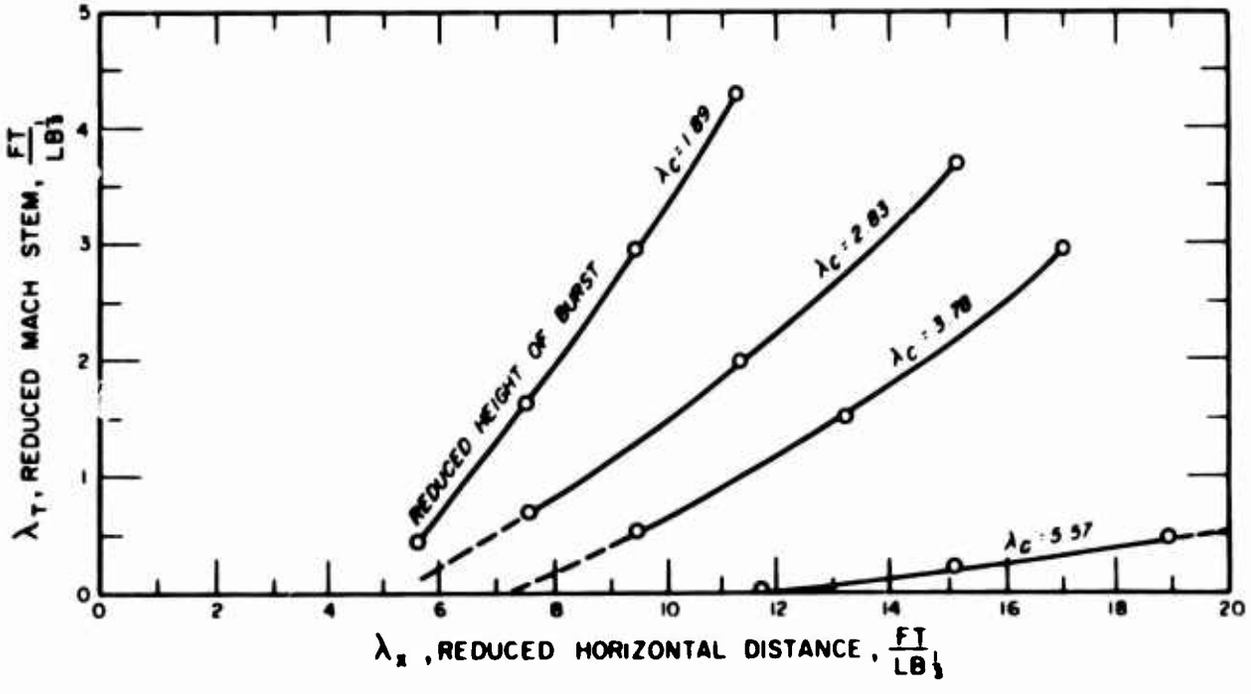

Figure 24. Length of Mach stem (or height of triple point) plotted against distance from ground zero for four different burst heights. The data are for small explosions over ice cap snow. (From Isgram, ref. 3)

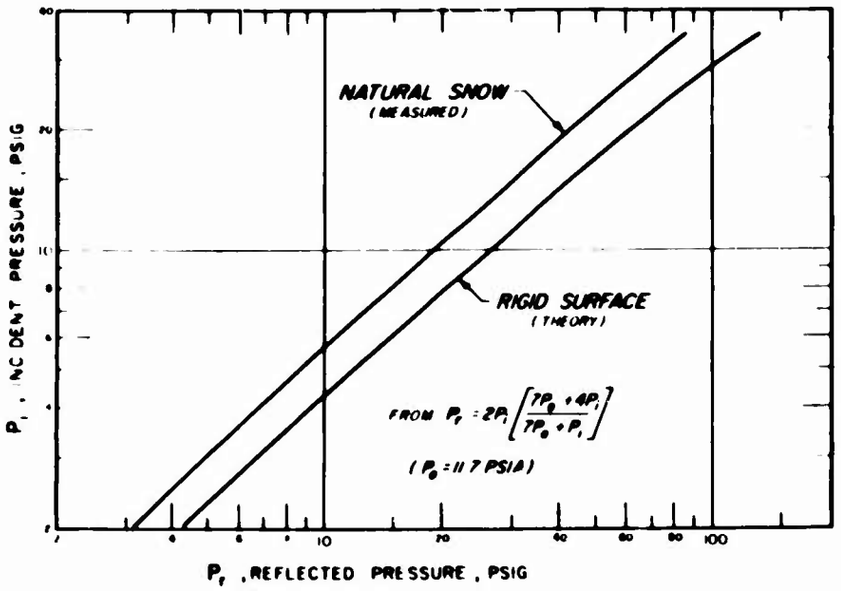

Figure 25. Reflected pressure versus incident pressure for air blast. The line summarizing data for a snow surface on the Greenland Ice Cap is compared with a theoretical relationship for a rigid surface. (From Ingram, ref. 3)

Overpressure and dynamic pressure. In assessing air blast effects it is necessary to consider, in addition to overpressure, the dynamic pressure, or wind pressure associated with the shock front travel.

In regions traversed by a single shock front (either a fused hemispheric wave from a surface burst or the Mach stem of an air burst) an equation for the shock velocity U can be derived[2].* Taking 1.4 as the ratio of specific heats for air the expression is

$$U = c_0 \left[1 + 0.857\left(p_m/P_0\right)\right]^{\frac{1}{2}} \qquad (19)$$

where c_0 speed of sound in the region ahead of the shock front

p_m peak overpressure

P_0 ambient pressure in the region ahead of the shock front.

Figure 26 compares shock velocity computed from eq 19 with shock velocities derived from direct observations for an air blast over snow.

The dynamic pressure is determined by the particle velocity, or wind velocity, u, behind the shock front ($\frac{1}{2}\rho u^2$, where ρ is air density behind the shock front). Velocity u and density ρ can be related to p_m, P_0, and c_0, leading to an expression giving the peak dynamic pressure q_m in terms of the peak overpressure p_m:

---

*Relevant theory is developed in standard texts on the flow of compressible fluids. Detailed treatment is given by Courant and Friedrichs in "Supersonic flow and shock waves" (Interscience, 1948).

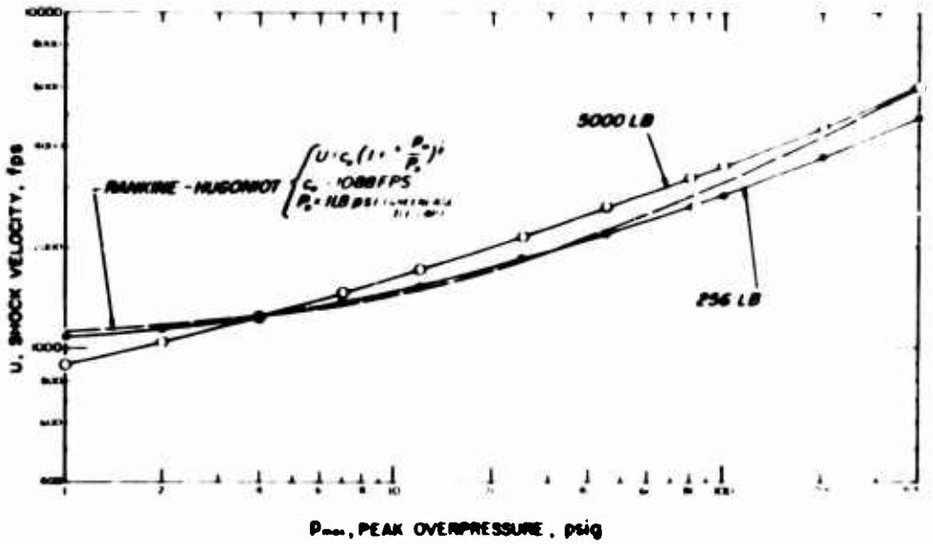

Figure 26. Relationship between shock velocity and peak overpressure, given by eq 19, for a typical ice cap location (P_0 - 11.8 psi). Results of tests made in Greenland are shown for comparison. Those results, obtained from measured pressures and arrival times, probably reflect calibration inadequacies (at small values of p_m for the 5,000 lb shot, U is lower than c_0). (After Smith, ref. 10).

$$q_m \quad \frac{2.5\, p_m^2}{7P_0 + p_m} \,. \tag{20}$$

Again a value of 1.4 for the ratio of specific heats is assumed.

Both overpressure and dynamic pressure have their maximum values at the shock front and, for a given location, both decrease to zero at about the same time (the positive phase of the dynamic pressure is actually slightly longer than that of the overpressure). Except in regions of very high overpressure ($p_m > 70$ psi), peak dynamic pressure is less than peak overpressure, and their rates of decay are therefore different. In regions of relatively low overpressure ($p_m < 10$ psi), the exponential decay of overpressure and dynamic pressure at a given point can be described by the empirical relations[2]

$$\frac{p}{p_m} \quad \left(1 - \frac{t}{t_+}\right) \exp\left(\frac{-t}{t_+}\right) \tag{21}$$

$$\frac{q}{q_m} \quad \left(1 - \frac{t}{t_+}\right)^2 \exp\left(\frac{-2t}{t_+}\right) \tag{22}$$

where p and q are the transient overpressure and dynamic pressure at time t, and t_+ is the positive phase duration.

Curves giving decay rates for a wide range of peak overpressures have been developed numerically, and these are reproduced in Figures 27 and 28. So far there is no experimental verification for pressures higher than a few hundred psi.

Information on the attenuation of peak overpressure with distance from a surface burst is usually drawn from empirical curves, although some theoretical considerations are in progress. In Figure 29 data are given for near-surface air blasts over snow produced by small H. E. charges (32 lb and 256 lb). The tests were made on the Greenland Ice Cap at a surface elevation of 6800 ft. On the same graph comparable data are given for a 1-kt nuclear explosion on snow-free ground andin a standard sea level

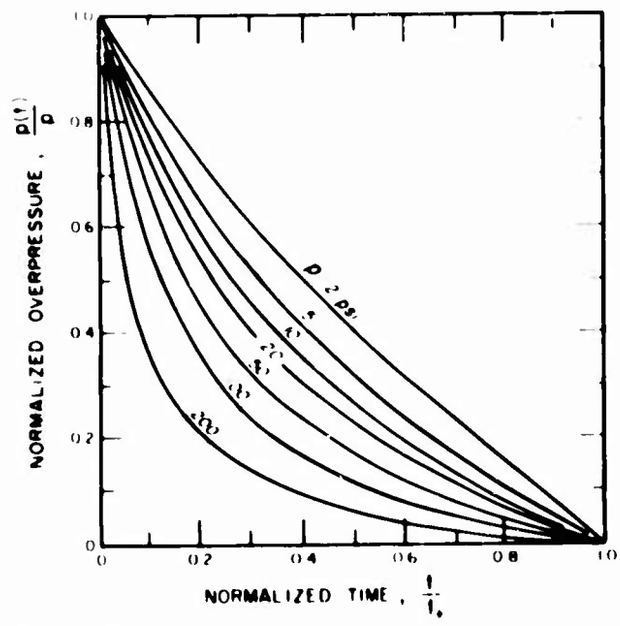

Figure 27. Decay of air blast overpressure with time for various values of peak overpressure. (After Glasstone, ref. 2)

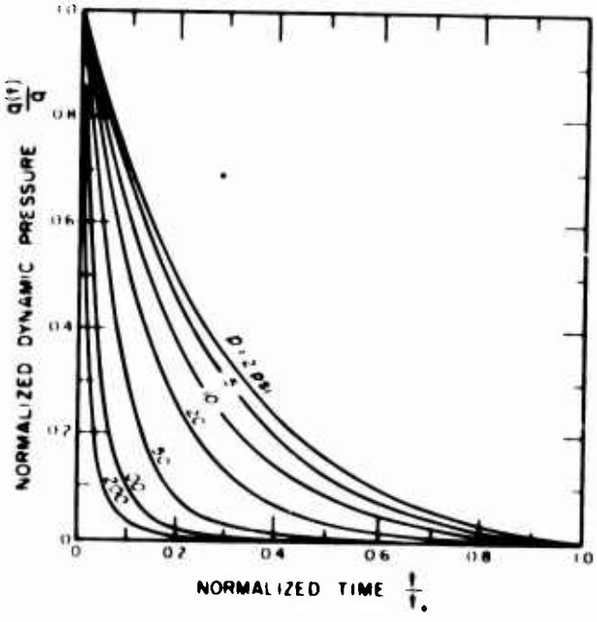

Figure 28. Decay of dynamic pressure with time for various values of peak overpressure. (After Glasstone, ref. 2)

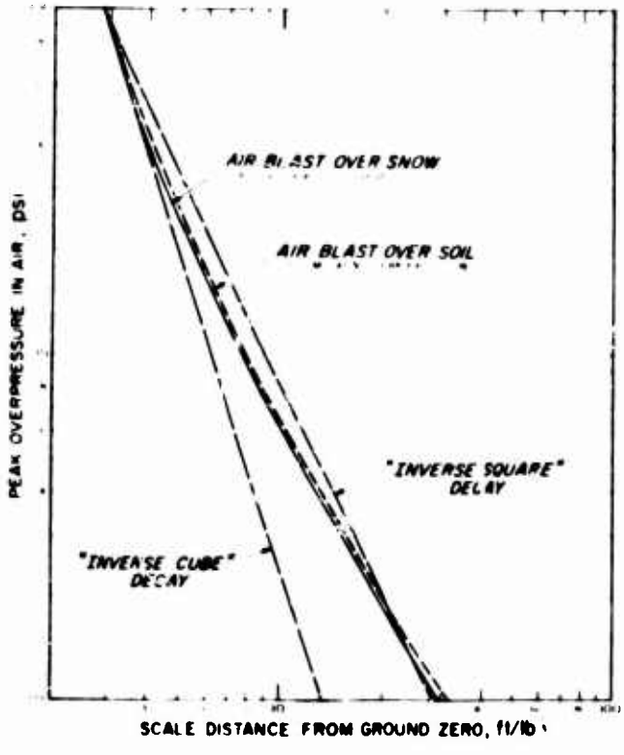

Figure 29. Relation between peak air overpressure and distance from ground zero. The full line gives data for contact H. E. bursts on snow. Charge weights were 32 lb and 256 lb and measurements were made on the Greenland Ice Cap at an altitude of 6800 ft (air pressure about 11.8 psi). The chain-dotted line is scaled from data for a 1-kt contact nuclear burst on snow-free ground at sea level. Scaling has been performed on the assumption that the 1-kt explosion is kinetically equivalent to 1 kt of TNT. (Oversnow data from ref. 3 and 10, nuclear data from ref. 2)

atmosphere. The 1-kt data are taken from ref. 2, and the distance has been scaled assuming the yield to be fully equivalent to 1000 tons of TNT. It is clear from the graph that power law approximations for decay of overpressure with distance must be used with caution; the "inverse cube" relation sometimes adopted ($p_m \propto 1/d^3$) seems valid only at the highest pressures (p_m >30 psi) and at short distances from the burst (scaled distance <5 ft/lb$^{1/3}$). Over the entire pressure range 1.0 to 100 psi, an inverse square relationship seems a reasonable approximation over a limited range centered on 12 psi.

A power law is a poor way to relate peak overpressure with distance; it might be more meaningful to use an expression analogous to eq 18, which provides a physically significant attenuation constant.

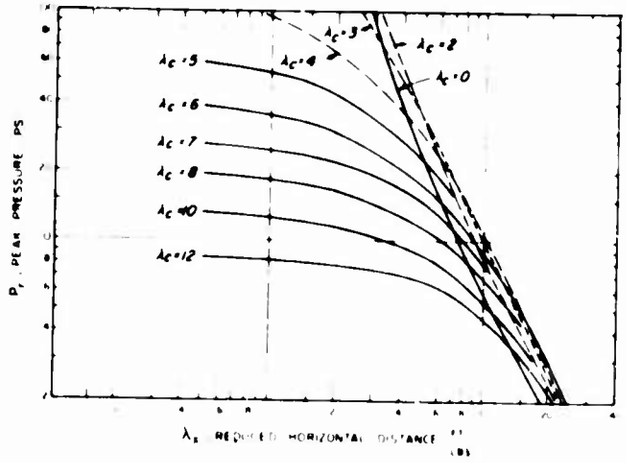

Figure 30. Peak overpressure as a function of horizontal distance from ground zero for blasts over snow. The parameter is burst height, and the symbol λ denotes scaled distances in $ft/lb^{1/3}$. Ambient pressure is 11.7 psi. (From Ingram, ref. 3)

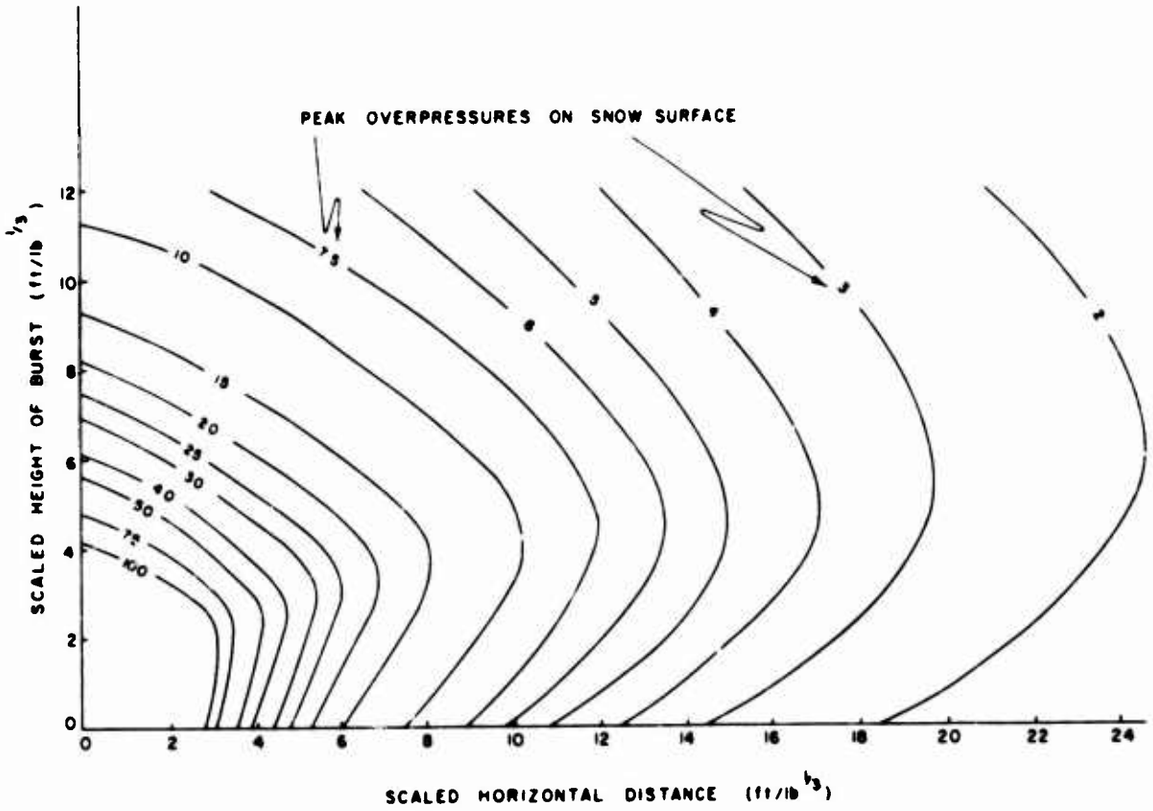

Figure 31. Peak overpressure related to height of burst and distance from ground zero for air blasts over snow. (Same data as Fig. 30.) (After Ingram, ref. 3)

In the case of a higher air burst the variation of overpressure with horizontal distance from ground zero takes a different form, as shown in Figure 30, where peak overpressure at the snow surface is plotted against scaled horizontal distance with scaled burst height as parameter. The same data are illustrated in a different form in Figure 31.

Influence of ambient atmospheric pressure and temperature. If air blasts are to be compared for widely different conditions of ambient air pressure and air temperature, then corrections for these changes must be made. This problem might arise in using the results of a blast experiment made at sea level to predict effects on a high ice cap or in the high mountains.*

The peak overpressure varies in direct proportion to the ambient air pressure[2] so that, at a given distance from the explosion, the ratio of overpressures for two different elevations is

$$\frac{p_2}{p_1} = \frac{P_2}{P_1} \tag{23}$$

where p is overpressure and P is ambient air pressure ahead of the shock front. Subscript 1 refers to the reference elevation and subscript 2 to the new elevation.

The distance (d) from the explosion at which a given peak overpressure is experienced is given by †

$$\frac{d_2}{d_1} = \left(\frac{P_2}{P_1}\right)^{\frac{1}{3}}. \tag{24}$$

This implies the questionable inverse cube assumption for decay of overpressure with distance. If the inverse square approximation is adopted instead, the exponent changes from $\frac{1}{3}$ to $\frac{1}{2}$.

Shock velocity varies with temperature and pressure, and the effect on arrival time and positive phase duration is given by

$$\frac{t_2}{t_1} = \left(\frac{P_1}{P_2}\right)^{\frac{1}{3}} \left(\frac{T_1}{T_2}\right)^{\frac{1}{2}} \tag{25}$$

where T is absolute temperature.

Blast impulse I is modified by temperature and pressure; the correction follows from eq 23 and 25 above:

$$\frac{I_2}{I_1} = \left(\frac{P_2}{P_1}\right)^{\frac{2}{3}} \left(\frac{T_1}{T_2}\right)^{\frac{1}{2}}. \tag{26}$$

Damage to undersnow structures

From the evidence on shock attenuation by snow, we may confidently expect that structures buried in deep (ice cap) snow will be well protected in comparison with structures buried in soil. In general, the considerations covering shock damage to structures in soils will apply to snow, although a ground shock in snow, whether initiated directly or by air blast, will decay with distance traveled more rapidly than

---

*This treatment refers to a wave traveling more or less horizontally. The problem of shock propagation from a high altitude air burst down to sea level is more complicated.

†The corresponding equation in article 3.60 of ref. 2, from which this information is taken, appears to have the cube root term inverted.

it would in most soils or in rock. One possible complication, which so far has not received much attention, is the possibility of damage by a wave refracted from deep ice (p. 16) at a structure which is safe from waves traveling more or less directly through the surface snow.* Structures in the rupture zones of craters (see above) will certainly be damaged.

Some undersnow facilities are contained within tunnels or shafts formed solely from snow. The most common of the pure snow structures is the cut-and-cover trench,[12] which is a tunnel formed by cutting an open trench and roofing it with an arch of milled snow (see Part III, Section A2). Tests have been made to determine the resistance of such structures to air blast, with favorable results. In a preliminary study[16,20] an arch of milled snow (9 ft span, 2 ft crown thickness) resisted 15 psi overpressures with only minor damage, while a thinner section of the same arch (6 in. crown thickness) withstood 10 psi. It was noticed that peak overpressures were lower than expected, suggesting that air blast energy was absorbed by the snow surface.[16]† Two types of arches were used in later tests:[11] true cast arches of 9-ft span, and "model" arches with vertically oriented crown axes, formed by drilling or digging holes of 6-108 in. diam in processed snow alongside an open trench. The model arches were unsatisfactory as representations of true horizontal arches (gravity forces were changed in direction, and blast reflections occurred in the open model trench), and withstood considerably less pressure than the true horizontal arches.

Figure 32 summarizes the results of tests on the vertical model arches, and shows the effect of variations in the ratio of arch span to crown thickness. The 9-ft span horizontal arches withstood about five times as much surface overpressure as the models, and 100-psi overpressure was sustained without complete failure by arches having 24 to 26-in. crown thicknesses.

It is now reported by Waterways Experiment Station that dimensional analysis shows the test charges to have been too small by a factor of 50 or more; to simulate response to weapons air blast, pulse duration must be matched to the natural period of vibration of the structure.

Charges have been detonated on the snow surface at various perpendicular distances from open snow trenches cut in the surface of the ice cap. It was found that explosions at scaled distances of 3 ft/lb$^{\frac{1}{3}}$ broke the trench walls (see Fig. 33). Bursts at a scaled distance of 4 ft/lb$^{\frac{1}{3}}$ caused major cracking in the trench walls, and at distances of 4-7 ft/lb$^{\frac{1}{3}}$ minor cracking occurred. Explosions further away from 7 ft/lb$^{\frac{1}{3}}$ caused no damage to the trench. As is shown by the crater relationships above, the radius of damage increases with charge depth for shallow shots, and therefore trenches will be damaged by bursts further away than 3-4 ft/lb$^{\frac{1}{3}}$ when the charges are suitably buried.

Some engineering uses of explosives in snow

Avalanche release. Explosives are used to trigger controlled avalanches and to break cornices which threaten to start avalanches. The particular way of using explosives is decided after assessing the prevailing snow and terrain conditions. There are three general methods for disturbing the snow: firing air or surface shots, firing charges buried in the snow, and firing charges buried in the underlying ground.

Air blasts spread the explosive disturbance over a wide area, in contrast to explosions within the snow cover, which are attenuated rapidly in a small radius. Charges fired inside the snow transfer maximum energy to the snow when deeply buried and tamped, but the shock effect is strictly localized. Explosions in the underlying ground give efficient energy transfer and spread the shock widely.

---

*It should be noted that simple scaling cannot be applied to this problem, since ice cap dimensions remain constant.

†It is also reported by Waterways Experiment Station that the high frequency response of the pressure gauges was inadequate.

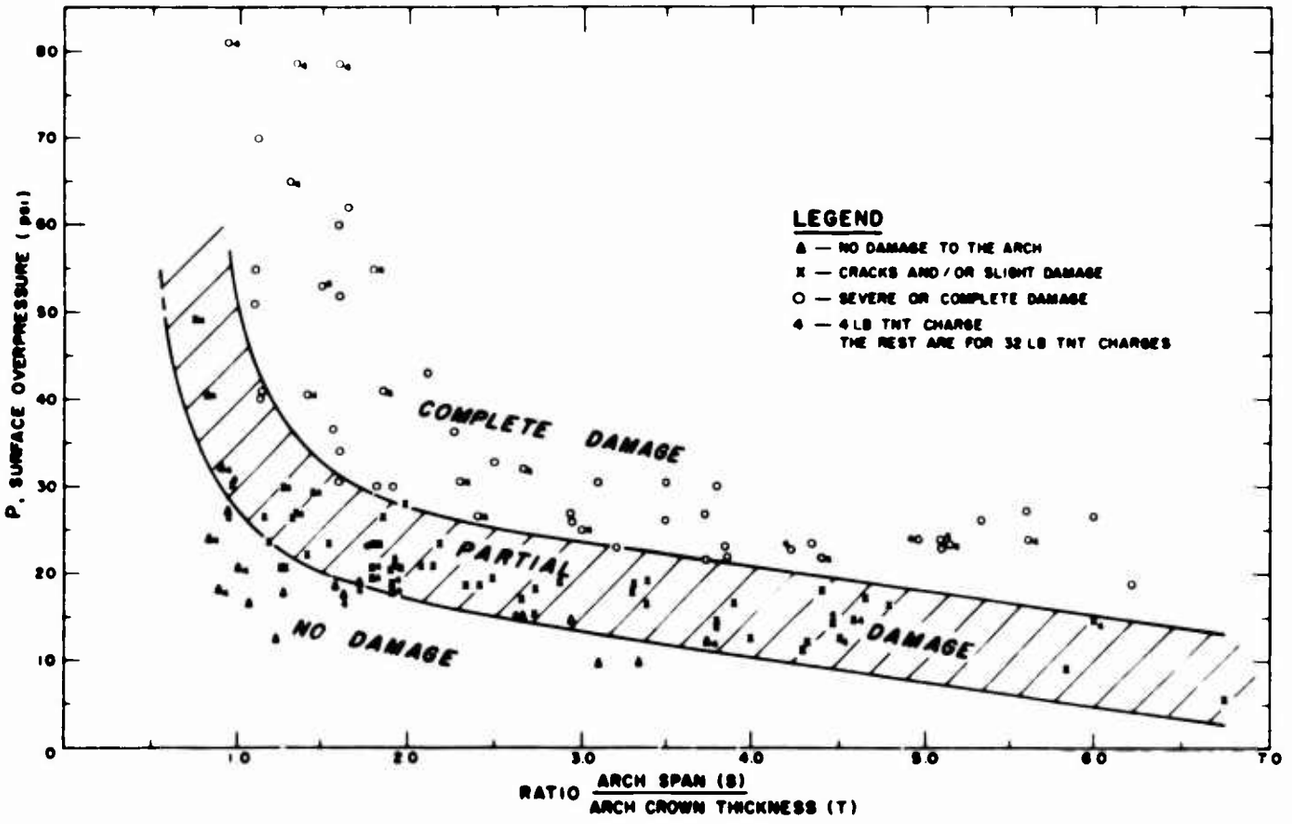

Figure 32. Summary of data for damage to model snow arches. Real arches withstood considerably higher overpressures than the model arches. (From Szostak and Benert, ref. 11).

Figure 33. Trench wall broken by a charge detonated on the surface at a scaled distance of 3 ft/lb$^{\frac{1}{3}}$ from the edge (Site 2, Greenland).

Some avalanche workers in the U. S. favor fast charges for releasing avalanches on slopes and more slowly burning powders for breaking cornices. In Europe, land mines are sometimes laid in critical avalanche zones before the snow falls and are later fired when danger develops. The use of explosive projectiles will be outlined in Part III, Section A3d, Avalanches.

Figure 34. Blowing the snow bridge of a crevasse near the edge of the Greenland Ice Cap during trail operations.

Crevasse blowing. Opening concealed crevasses by blowing their snow bridges is standard military practice in polar sled train operations (Fig. 34). Explosives used in U. S. Army operations are "composition" C-3 and C-4 and 30-40% dynamite. Composition is highly stable at all temperatures and dynamite is stable but to a smaller degree. Composition is molded into shaped charges, or is mixed with engine oil in ratios up to one part oil to two parts explosive by weight. Oil mixtures are contained in number $2\frac{1}{2}$ or number 10 cans.

The first hole is blown in the snow bridge by augering a 3 in. diam hole and charging it with either seven sticks of dynamite, two 3-lb sticks of C-3/C-4, or two number $2\frac{1}{2}$ cans of composition-oil mixture.

Further opening of the bridge is effected by firing a line of shots at 7-ft centers along the line of the crevasse. The shot holes are positioned and the charge weights chosen after consideration of the situation revealed by the first explosion. The cornices, or snow bridge haunches, at the crevasse edges must be destroyed, and this usually entails a line of shots along the extreme edge of the bridge.

Ramping cliffs. It is sometimes necessary to cut a ramp in a vertical cliff of dense snow or ice to permit vehicle access or to provide discharging facilities for ships. Explosives can be used to split off a wedge of ice and the ramp can be finished by blading with a bulldozer.

Figure 35. Cut-and-cover trench (with thin arch roof of Peter snow) destroyed by a 30-lb charge fired inside the trench.

For a cliff of snow-ice (e.g. the edge of an Antarctic ice shelf) Benert (private discussion) estimates that charges should be a scaled distance of 5 ft/lb$^{\frac{1}{3}}$ from the edge of the cliff, and that they should be buried to a scaled depth of 5 ft/lb$^{\frac{1}{3}}$ also. This estimate is supported by the cratering data above. The actual depth of burial (and also the distance from shot hole to cliff edge) should probably be about half the height of the cliff.

The charge weight can be calculated from

$$\text{charge weight (lb)} \quad \left(\frac{\text{actual charge depth}}{\text{scaled charge depth}}\right)^3 = \left(\frac{\frac{1}{2} \times \text{cliff height in ft}}{5}\right)^3.$$

Excavation. Explosives are not likely to be needed for loosening snow in general engineering excavation when mechanical equipment is available, although they may be useful when hand digging is employed in snow interspersed with ice lenses. Explosives may sometimes be used to assist in clearing high banks of drifted snow or avalanche debris (particularly if the avalanche debris has rock and soil mixed with the snow). The crater relationships provide a guide for choosing size, depth and spacing of charges.

Demolition. For demolition of a "hard" structure on a polar snowfield, charges should be attached directly to the structure and not placed in snow adjacent to it. Snow tunnels and roofed trenches can be destroyed most effectively by firing charges inside the tunnels. A 30-lb charge will wreck a considerable length of newly constructed cut-and-cover trench when detonated inside (Fig. 35).

Seismic exploration. Small charges are used to generate elastic waves for seismic exploration, both air shots and subsurface shots being utilized. Deeply buried charges give the most efficient energy transfer in high-density ice cap snow, but air shots are occasionally preferred for technical reasons (see Part II, Section A2, Exploration geophysics).

LITERATURE CITED

1. Fuchs, A. (1957) Effects of explosives on snow, U. S. Army Snow Ice and Permafrost Research Establishment (USA SIPRE) Special Report 23.
2. Glasstone, S. (Editor)(1962) The effects of nuclear weapons, Dept. of the Army pamphlet no. 39-3.
3. Ingram, L. F. (1962) Air blast in an arctic environment, U. S. Army Waterways Experiment Station, Technical Report no. 2-597.
4. _____ (1960) Measurements of explosion-induced shock waves in ice and snow, Greenland, 1957 and 1958, U. S. Army Waterways Experiment Station, Miscellaneous paper no. 2-399.
5. Jones, G. H. S. (1962) Some comments on cratering, Suffield Experimental Station, Defense Research Board, Canada, Suffield special publication 22.
6. Livingston, C. W. (In prep.) Explosions in snow, U. S. Army Cold Regions Research and Engineering Laboratory (USA CRREL) Technical Report 85.
7. Mellor, M. (1964) Properties of snow, Cold Regions Science and Engineering (F. J. Sanger, Editor), USA CRREL Monographs, Part III, Section A1.
8. Nakaya, U. (1959) Visco-elastic properties of snow and ice from the Greenland Ice Cap, USA SIPRE Research Report 46.
9. Plump, R. (1963) A tentative appraisal of the effects of snow and ice on a nuclear explosion, USA CRREL Review Note (internal).
10. Smith, N. (1962) Air pressures and shock wave velocities from high explosive surface contact explosions over Arctic snow surface, USA CRREL Technical Note (unpublished).
11. Szostak, H and Benert, R. (In prep.) Destruction of snow structures by explosives, USA CRREL Technical Report 92.
12. Waterhouse, R W (1960) Cut and cover trenching in snow, USA SIPRE Technical Report 76.
13. U. S. Army (1955) Military explosives, TM 9-1910, Washington.
14. _____(1954) Explosives and demolitions, FM 5-25, Washington.
15. DuPont de Nemours and Co.(Inc.)(1958) Blasters' handbook, Wilmington.
16. Ingram, L. F. (1960) Blast effects on a snow tunnel, Camp Century, Greenland, U. S. Army Waterways Experiment Station, Miscellaneous Paper no. 2-378.
17. _____ and Strange, J. N. (1958) Blast-pressure measurements in snow, U. S. Army Waterways Experiment Station, Miscellaneous Paper no. 2-274.
18. Joachim, C. E. (1964) Structures in an arctic environment, U. S Army Waterways Experiment Station, for Defense Atomic Support Agency, Technical Report no. 1-649, Report 3. (Also Report 2, Dynamic tests on snow structures, in preparation.)
19. Livingston, C. W. (1960) Explosions in ice, USA SIPRE Technical Report 75,
20. McCoy, J. E and Waterhouse, R W. (1960) Effects of a shock wave on a Peter snow arch, USA SIPRE Special Report 39.
21. Napadensky, H. (1964) Dynamic response of snow to high rates of loading, USA CRREL Research Report 119.

REFERENCES (Cont'd)

22. Sager, R. A., Denzel, C. W., and Tiffany, W. B. (1960) Compendium of crater data, U. S. Army Waterways Experiment Station, Technical Report no. 2-547, Report 1.

23. Strange, J. N., Denzel, C. W., and McLane, T. I. (1961) Analysis of crater data, U. S. Army Waterways Experiment Station, Technical Report no. 2-547, Report 2.